E81-10138
CR-164122

NCC 5-22

An Investigation of Vegetation and Other Earth Resource/Feature Parameters Using Landsat and Other Remote Sensing Date

I. Landsat

II. Remote Sensing of Volcanic Emissions

Semi-Annual Status Report (#2)

August 1, 1980 to January 31, 1981

Dartmouth College

Hanover, NH 03755

Principal Investigators:

Richard W. Birnie, Assistant Professor of Geology

Richard E. Stoiber, Emeritus Professor of Geology

Researchers:

Emily Bryant, Senior Research Assistant

A. G. Dodge, Area Forester, Cooperative Extension Service (UNH)

Kevin Doran, Assistant Grafton County Forester (UNH)

Tom Stone, graduate student

David Sussman, graduate student

Lawrence Malinconico, graduate student

Stanley Williams, graduate student

Undergraduate Student Assistants

(E81-10133) AN INVESTIGATION OF VEGETATION AND OTHER EARTH RESOURCE/FEATURE PARAMETERS USING LANDSAT AND OTHER REMOTE SENSING DATA. 1: LANDSAT. 2: REMOTE SENSING OF VOLCANIC EMISSIONS Semiannual Status (Dartmouth   N81-22449

Unclas
G3/43 00133

Dartmouth College

Semi-Annual Status Report - NCC 5-22

August 1, 1980 - January 31, 1981

This report covers activities of the Landsat Sensing Research Group (Earth Resources) and of the Volcanic Gas Sensing Research Group (Planetary Science) which work in collaboration with the Goddard Institute for Space Studies, New York; Dr. Robert Jastrow, Director. Dr. Stephen Ungar of GISS is the Technical Officer for this project.

NCC 5-22 supports work which was started in 1974 under NSG 5014. The work described below I. B., (Geology and Geobotany) will in the future be supported under another Cooperative Agreement or Grant.

I. Landsat

The Dartmouth Landsat Research Group continued application studies for Landsat data under the general category of analysis of vegetation cover, especially forestry and geobotany, that is, the effects of soil/earth mineral content on vegetation.

A. Forestry

I. Introduction

In the past half year, we have had some changes in personnel, have worked on applications of Landsat data, developed applications techniques, and have maintained and established contacts with remote sensing colleagues. We have noticed an increased awareness of and interest in the use of Landsat data in New England:

II. Changes in Personnel

Kevin Doran has replaced Ken Sutherland as forestry advisor from the UNH Cooperative Extension Service and has quickly taken hold of these responsibilities. Emily Bryant has entered the Computer and Information Sciences Program as a Master's candidate and has been working on this project half time. Gibb Dodge's role has remained the same. Undergraduate assistants were Mark Heuberger (fall), and Sally Johnson and Paul Fisher (winter).

III. Applications Projects

A. Investigation of the fanning algorithm as applied to Maine forests was completed, written up as an abstract, submitted, and accepted as a poster for the 15th ERIM Symposium in May, 1981. (Enclosure 1)

B. Deer yard habitat. Mark and Kevin field-checked areas in southwestern New Hampshire which the NH Fish and Game Department had indicated were deer yards. Mark used these areas (largely softwood) to develop signatures for potential deer yard habitat. In a field trip to Canaan, signs of deer were found in two out of four or five areas that had printed out as deer yard. Printouts of three towns in southwestern NH were made with these signatures. Reaction from the Fish and Game Department was positive. We are refining these signatures and developing output appropriate to their needs (e.g. overlays of topography).

C. Gypsy moth defoliation mapping. Tapes were finally acquired, but since they are in the wrong format, there is a delay in using them.

D. Recent report by Cooperative Extension Service (sub contract) is at Enclosure 2.

IV. Techniques

We are writing a program on the Dartmouth computer to calculate pixel coordinates given latitude and longitude and vice versa. Mark determined ground control point coordinates for a significant portion of New Hampshire; Em and Paul have been writing code for the program.

V. Maintaining Contacts - spreading the word.

Em went to GISS in September to meet with Arch Park in regards to his project mapping biomass.

Gibb, Em, and Kevin attended the RSGNNE meeting in Burlington in September.

Gibb and Em gave a guest lecture for Dave Lingren's (Geography) remote sensing class.

Kevin and Em met with Kurt Olson (UNH) to see how his work is going and to catch up on news.

At our invitation, Helen Mustafa and Bob Edwards from the New England Area Remote Sensing System (NEARSS) visited Dartmouth. We discussed NEARSS and remote sensing in New Hampshire.

Gibb, Kevin, and Em visited Bob Barker of St. Regis Paper Company in Jacksonville, Florida. We saw their Forest Resource Inventory System which is being put together now. It incorporates Landsat data as one of many levels of information in their forest inventory.

Article "Landsat for Practical Forest Type Mapping: A Test Case" was (finally) published in Photogrammetric Engineering and Remote Sensing Magazine, December, 1980. (Reprint, Enclosure 3)

VI. Increased Awareness.

Over the past year or so, a number of projects involving Landsat have cropped up in New England. A Landsat Demonstration

Project backed by ERRSAC has been initiated in New Hampshire. Maine has a similar project started within the last year. Vermont's demonstration project has been underway for a couple of years. The NEARSS group, whose concern in largely with access to real-time ocean and coastline remote sensing data, started gathering information and making plans last spring. The New England Inovation Group (funded by NSF) has a contract from NASA Headquarters to investigate the use of Landsat data on the local and regional government level. All in all, things are starting to cook!

B. Geology and Geobotany

The geobotany group have been involved in refining the data collected over the Mesatchee Creek prospect. A Chi squared statistical test was applied to the aircraft multispectral scanner data and it confirmed the extremely high correlation (>99.9%) of the anomalous spectral data to the mineralized zone. This data has been included in a revised paper sent to Economic Geology. (see previous semi-annual report) This paper has been accepted for publication.

II. Remote Sensing of Volcanic Emissions

This research group consists of Professor Richard Stoiber and Graduate Assistants Lawrence Malinconico, Stanley Williams (Ph.D. candidates) and David Sussman. During the period of this report (August 80 - January 81) they were concerned with:

a. Mt. St. Helens Eruptions including the RAVE Mission.

b. Monitoring volcanic activity in Nicaragua, El Salvador and Guatemala (Foreign travel supported by others)

c. Testing a Mini-Cospec.

d. Reporting various activities at Scientific Meetings.

1. Mt. St. Helens

The RAVE Mission is described in Enclosure 4. Professor Stoiber participated with the group, in the remote sensing of SO_2. This report was presented at a symposium on the Mt. St. Helens Eruption in Washington, DC, November 18-19, 1980 (Enclosure 5). At this meeting, a paper was presented (Enclosure 6) to which Stoiber, Malinconico and Williams contributed. A similar paper was presented at the 1980 AGU Fall Meeting (see below and Enclosure 8, V 39).

2. The group visited Central America again in November - December, 1980. This activity continues the field proofing of the Mini-Cospec loaned by Barringer Research, the manufacturer, Toronto, Canada. The field expenses, including travel, for this work, are supported by others (esp NSF) but the work contributes generally to the expertise and reputation of the group. Recent activities have been reported in the SEAN (Scientific Event Alert Network of the Smithsonian Institution) Bulletin #12, Dec. 31, 1980 (Extract at Enclosure 7) and at the 1980 AGU (American Geophysical Union) Fall Meeting Dec. 10-15, 1980 in San Francisco (Abstracts of 3 papers V 132, V 133, V 136, Enclosure 8).

Encl. 1-8, a/s

Fanning: A Classification Algorithm for Mixture Landscapes Applied to Landsat Data of Maine Forests

Stephen G. Ungar and Emily Bryant

I. Introduction

Most Landsat classification algorithms used today separate land cover into discrete categories on the basis of presence or absence of a land cover type: "wheat vs. non-wheat". Most landscapes, however, include a mixture of types: trees plus grass in an orchard, or corn plus soy along a field boundary. These would be better classified on the basis of the proportion of the area covered by each type. The "fanning" algorithm was developed at the Goddard Institute for Space Studies by Stephen Ungar, to accomodate mixture landscapes. It quantifies the varying proportions of two "pure" land cover types within a pixel.

II. Description of Algorithm

Assume each pixel to be composed of a mixture of cover type A and cover type B. "Pure" pixels of cover type A have a mean spectral signature specified as A_1, A_2, A_3, A_4 where A_i is the energy received at the satellite in the ith spectral band. The energies in each of the four Landsat MSS bands may be thought of as the components of a 4-dimensional observation vector $\vec{A}$. In a similar manner $\vec{B} = (B_1, B_2, B_3, B_4)$ represents the spectral signature of a "pure" pixel of cover type B. In principle, the signature of a pixel composed of a mixture of cover types A and B may be expressed as

$$\vec{S} = \eta\vec{A} + (1 - \eta)\vec{B}$$

Enclosure 1

where η represents the fractional area occupied by cover type A. As η varies from 0 to 1 a "fan" of vectors is formed, ranging in direction from $\vec{B}$ to $\vec{A}$ and terminating on the line joining $\vec{B}$ and $\vec{A}$.

In a real situation, the observed signature of a mixture pixel will generally not terminate on this line. Our technique determines which value of η minimizes the difference between observed signature and a theoretical signature terminating on the line. Geometrically, this is equivalent to finding the end point of the theoretical mixture vector by dropping a perpendicular from the observed signature to the line joining the pure types.

The problem may be analytically stated as follows:

If, $\delta S = |\vec{S}_{obs} - [\eta\vec{A} + (1 - \eta)\vec{B}]|$; find η such that $\frac{\partial}{\partial\eta}(\delta S) = 0$. The formal solution is simply the least squares fit determination of η among the four values obtained by considering each Landsat band independently.

The fanning algorithm is available in both an unsupervised and supervised mode. In the unsupervised mode, the GISS chaining algorithm is used to allow pixels to chain together into clusters and fans. The algorithm selects the signatures for the pixel pair with the largest separation in each fan as the endpoints or "pure" types. A value of η is then determined for each remaining pixel in the fan in terms of these pure types. In the supervised mode, the user specifies the pure type signatures which are applied to a category of pixels defined from some previous supervised or unsupervised classification.

In both modes, the algorithm tests: (a) the value of η derived for each pixel for physical reasonableness (i.e., $0<\eta<1$, if the fractional area hypothesis for a two component mixture is correct); and (b) the goodness of fit of the observed signature to the fan (i.e., $\delta S \approx 0$ if the observed vector is close to a theoretical vector lying in the fan).

This study uses only the supervised mode.

III. Application of the Fanning Algorithm in Forestry

One goal of the Earth Resources Group at GISS is to make useful forest type maps with Landsat data. Forest types used in current practical forest inventories in the northeastern U.S. are defined by the proportion of hardwood (deciduous) and softwood (evergreen) trees in an area. Definitions and their interpretation vary from user to user. If the fanning algorithm could provide objective and consistent quantification of forest type proportions, Landsat maps could meet or even surpass users' inventory specifications.

IV. Results to Date

As a test of the fanning technique, a classification was compared with a detailed inventory of ½ million acres of forest land in northern Maine, managed by the Seven Islands Land Company, Bangor, Maine. Landsat data was recorded in August, 1976. The inventory, done the same year, breaks out four general forest types:

Type	H/S Ratio
Hardwood	100/0 to 75/25
HS	75/25 to 50/50
SH	50/50 to 25/75
Softwood	25/75 to 0/100

A scale for the fan was set up where 0.0 represented pure hardwood and 1.0 pure softwood. One would expect, therefore, to partition the forest types at values of 0.25, 0.50, and 0.75 on the scale. To match inventory acreages on the 29 subareas (townships) of the applications area, however, the scale had to be partitioned at mean values of 0.294 (± 0.046), 0.536 (± 0.044), and 0.642 (± 0.043). Although these values were significantly different from expected, they were consistent across the applications area. This suggested that actual partition values could be determined quite confidently from a sample area. The partitioning determined from two sample townships (10% of the area) was used to make acreage estimates for the four forest types in the applications area. Differences between classification and inventory were within 5½% over the area as a whole, and within an average of 22% by township. These differences are similar to those observed in a classification of the same area using a "discrete categories" algorithm.

To test temporal consistency, the fanning algorithm was also applied to Landsat data from July, 1976. Over an application area which was limited by clouds, August partition values were 0.271, 0.522, and 0.638; July values were 0.212, 0.500, and 0.647. Slope of the regression line between dates was close to 1, and correlation was high (0.997).

It can be concluded from the project that the fanning algorithm provides consistent quantification of mixtures of two forest types. Partition values for specific ratios of pure types, however, have to be derived empirically at this point.

V. Advantages of Approach

Several approaches which treat pixels as two component mixtures have appeared in the literature. Two strong points of the GISS approach are:

1) The technique is based on a simplistic physical model rather than a statistical approach, and readily allows for improvement by model refinement (e.g., a more recent version of the algorithm takes into account shadowing and slope effects by permitting the fractional areas of the two components to sum to less than one).

2) In unsupervised mode "pure" type signatures are extracted for the end points in a group of pixels and the mixture ratio is determined for each remaining pixel in terms of these pure types. The algorithm automatically rejects pixels which are inconsistent with the two component mixture hypothesis.

The practical application outlined in this paper provides perhaps the first quantitative evaluation of a mixture classification algorithm for large area inventories.

PROGRESS REPORT

APPLYING LANDSAT MEASUREMENTS

TO FOREST RESOURCE INVENTORIES

May 31, 1980 through December 31, 1980

Kevin Doran and Gibb Dodge, Cooperative Extension Service, coodinated their activities with Emily Bryant, Dartmouth College and other representatives of GISS.

SITE SELECTION

1. Finished developing field maps of deer yard areas in the towns of Washington, Stoddard and Henniker for the N.H. Fish and Game Department. Will deliver to the Department and test usefulness.

2. Select gypsy moth defoliation training sites.

3. Select new spruce-fir defoliation training sites

GUIDANCE AND EVALUATION

a) GISS on making changes in computer programs to produce better products continued.

b) Dartmouth work-study students - mapping techniques, observing ground truth sites, development of rotation and scale change program.

c) Private landowners with large ownership - using computer maps as field tools

d) Revise and update 1981 work plans

e) Evaluation - analyze computer outputs resulting from GISS program changes

COLLABORATION

1. Serving on Cooperative Extension Service National Task Force for remote sensing - advice to Extension Committee on policy related to Extension activity in remote sensing technology transfer.

2. Update information to the University of Vermont, University of New Hampshire, Maine Forestry Group, GISS, ERRSAC, GSFS, Remote Sensing Group of Northern New England, New Hampshire Fish and Game Department and Office of State Planning and NEARS personnel.

3. Remote sensing meetings with University of New Hampshire and Office of State Planning, and Dartmouth.

4. Met with N.H. Office of State Planning personnel on New Hampshire Landsat demonstration project with ERRSAC.

Enclosure 2

TECHNOLOGY TRANSFER AND REPORTING

1. Landsat presentations to classes of Dartmouth

2. Generate remote sensing technology to New Hampshire Fish and Game Department and Division of Forests and Lands.

SUBMITTED BY:

Kevin Doran, Program Assistant

Arthur "Gibb" Dodge, Jr.,
Program Leader

EMILY BRYANT
Department of Earth Sciences
Dartmouth College
Hanover, NH 03755
and NASA/Goddard Institute for Space Studies
New York, NY 10025
ARTHUR G. DODGE, JR.
Cooperative Forestry Programs
Cooperative Extension Service
University of New Hampshire
Durham, NH 03824
SAMUEL D. WARREN
Seven Islands Land Company
Bangor, ME 04401

Landsat for Practical Forest Type Mapping: A Test Case

Computer classified Landsat maps agreed to within 5 percent of a conventional inventory of forest lands in northern Maine.

INTRODUCTION

MANY PEOPLE have used Landsat data in mapping natural resources and cultural features (Bauer *et al.*, 1978; Dejace *et al.*, 1977; Gaydos and Newland, 1978; George *et al.*, 1977; Krebs and Hoffer, 1976; Mukai and Takeuchi, 1979; Odenyo and Pettry, 1977). In particular, researchers across North America have reported use of Landsat data in mapping forest resources (Beaubien, 1979; Dodge and Bryant, 1976; Harding and Scott, 1978; Johnson *et al.*, 1979; Kalensky *et al.* 1979; Kirby *et al.*, 1975; Kourtz, 1977; Mead and Meyer, 1977; Sayn-Wittgenstein, 1977; Titus *et al.*, 1975; Williams and Haver, 1976).

The goal of the Dartmouth forestry section of the Goddard Institute for Space Studies is to use computer classification of Landsat data to make forest type maps which are useful to the field forester. Thus, the person who cruises the forest rather than the upper level manager is the "user" for whom the Landsat maps are being developed.

ABSTRACT: *In a cooperative project, computer classified Landsat maps were compared with a recent inventory of forest lands in northern Maine. Over the 196,000 hectare (485,000 acre) area mapped, estimates of area of softwood, mixed wood, and hardwood forest types by the two methods agreed to within 5 percent. Cost of the Landsat maps is estimated at 6.5 cents per hectare (2.6 cents per acre). Although the information derived from Landsat is not yet refined enough to be incorporated in current forest inventories, the techniques used are worth developing.*

SEVEN ISLANDS PROJECT

The Seven Islands project developed from a contact with a potential Landsat data user employed by the Seven Islands Land Company, Bangor, Maine. Seven Islands manages 690 thousand hectares (1.7 million acres) of forest land in northern Maine and New Hampshire. They require information about forest types on their lands for management decisions and for taxation purposes. (The state of Maine taxes forest land by applying different values to softwood, mixed wood, and hardwood forest areas.) A detailed inventory of the Seven Islands lands was underway at the time the contact was made. This presented a rare opportunity to test Landsat's ability to meet practical user information needs: the user requirements were well defined (in the inventory specifications) and there was a product, the standard inventory, against which to measure Landsat mapping performance.

With the cooperation of the Seven Islands Land

PHOTOGRAMMETRIC ENGINEERING AND REMOTE SENSING,
Vol. 46, No. 12, December 1980, pp. 1575-1584.

Enclosure 3

Company, a project was started. The goal was to match their inventory specifications as closely as possible using computer classification of Landsat data, and to create, quickly and inexpensively, a product suitable to submit to the Bureau of Taxation. There is a difference between this and some other Landsat applications projects. Success is measured by agreement with a given inventory, not by agreement with "ground truth" gathered by the Landsat investigators. A positive aspect of this approach is the elimination of biases which Landsat investigators might introduce in gathering their own ground truth.

More specific goals of the project were

- To map the Ashland District portion of the Seven Islands lands (Figure 1);
- To match computer-classified Landsat categories with Seven Islands inventory categories: softwood, mixed wood, and hardwood forest types, non-forest areas, water, and roads;
- To calculate area for each category in each Seven Islands management unit (units are usually townships or parts of townships); and
- To produce geometrically corrected computer printout maps of the area at 1:24,000 scale.

The following constraints were put on the project in order to approximate an operational situation:

- Minimize the amount of ground truth used in creating and checking the Landsat classification (methods dependent on large amounts of ground truth are suitable only for research situations, and
- Keep track of expenses—human and computer time, cost of data and supplies—to give an estimate of cost per unit area.

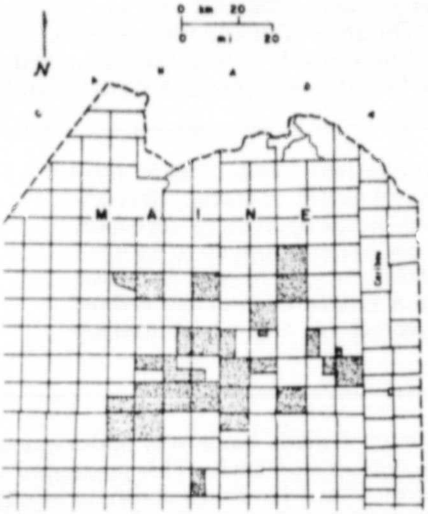

FIG. 1. Ashland District portion of Seven Islands Land Company lands, an area of about 196,000 hectares (485,000 acres). Individual parcels are not always contiguous and range in size from 400 to 10,500 hectares (1,000 to 26,000 acres).

THE ASHLAND DISTRICT

The Ashland District, managed by Seven Islands Land Company, consists of land in 29 townships in northern Maine located between 46 and 47 degrees north latitude. In most of the area, the political subdivisions are "unincorporated townships" where there is very little permanent human settlement.

The individual parcels or townships in the Ashland District are not always contiguous and range in size from 400 to 10,500 hectares (1,000 to 26,000 acres). The District comprises a total of 196,356

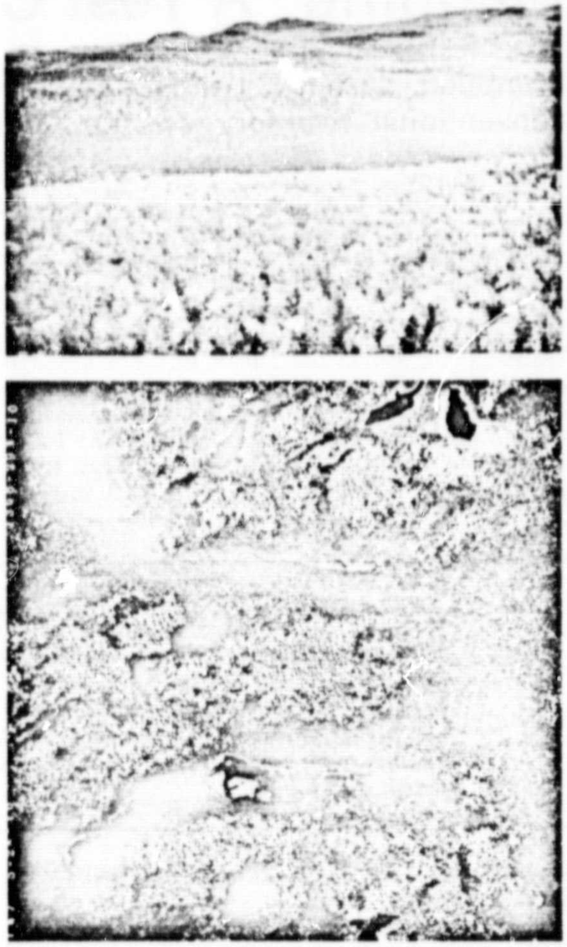

FIG. 2. Oblique (above) and vertical (below) views of a portion of the Ashland District. The vertical view is an example of the black-and-white infrared photos used in the Seven Islands inventory (original scale 1:15,840; photos taken in May, 1976).

hectares (485,310 acres) (Figure 1). The most common forest types in this area are

- spruce-fir (*Picea sp.—Abies balsamea*)
- maple-beech-birch (*Acer saccharum—Fagus grandifolia—Betula alleghaniensis*)
- northern white cedar—black spruce (*Thuja occidentalis—Picea mariana*)

Figure 2 shows oblique and vertical views of part of the Ashland District.

THE SEVEN ISLANDS INVENTORY

The Seven Islands inventory is based on aerial photo-interpretation, "3-P" (probability proportional to prediction) field sampling, and the STX computer program (a standard forest measurement program). Figure 2 includes an example of the photos used in the inventory. The inventory consists of type maps, acreage tallies, and volume estimates. This project concentrated on matching the maps and acreage tallies, leaving volume estimation to other techniques.

The Seven Islands maps distinguish vegetation by type, size, and density to a 10 acre minimum. Acreage is determined for each forest stand, and totals are computed by type for each township. For tax purposes, the many forest types distinguished in the inventory are grouped into three more general types according to the proportion of softwood (conifer) to hardwood (deciduous) trees in an area:

- softwood—at least 75 percent of the trees are softwood.
- hardwood—at least 75 percent of the trees are hardwood.
- mixed wood—the proportion of softwood to hardwood trees lies between those of the softwood and hardwood categories as defined above.

The above are the general forest categories that were to be matched in the Landsat classification.

PROCEDURE

GENERAL OUTLINE

The project employed computer programs to make maps and acreage tallies from Landsat multispectral scanner (MSS) digital data. A supervised classification approach was used. It was developed at the Goddard Institute for Space Studies (GISS) by Stephen G. Ungar and is described in Merry *et al.* (1977). With the GISS classification algorithm, the program user defines a volume in four-dimensional color space around an average signature for each land cover category. The signature is usually the average reflectance of a land cover type as taken from a representative sample of the MSS data (a "training site"). The user can create a classification category for which there is no training site, if there is another source of signatures.

FIG. 3. MSS band 6 image of the 11 August 1976 Landsat scenes used in classifying the Ashland District (scene identification numbers 5480-14040 and 5480-14043). Ashland District is outlined; sample townships are labeled 1 and 2. Water is black, softwood dark gray, and hardwood light gray.

DETAILS OF THE SEVEN ISLANDS PROJECT

Landsat data used in the Seven Islands project was recorded on 11 August 1976. Scene identification numbers are 5480-14040 and 5480-14043 (Figure 3).

Ground truth consisted of

- Representative copies of the photos used in the Seven Islands inventory (Figure 2);
- Seven Islands inventory maps and acreage tallies for two of the 29 townships in the District;
- Personal knowledge from an overflight of the area;
- Prints of photo-mosaics used for location of forest harvests (scale 1:31,680); and
- Topographic maps (scale 1:62,500).

There was no ground checking except indirectly through the inventory information.

We chose signature training sites in the MSS data (usually 10 to 30 pixels in size) for softwood, hardwood, water, bog, and open categories using the aerial photographs. Mixed wood signatures were made by interpolating between hardwood and softwood signatures.

The tolerance parameters for the forest categories were adjusted so that the acreage tallies would agree with the Seven Islands inventory on two sample townships (Table 1). Discrepancy in acreage figures on the two townships taken together was under 3.5 percent; it was under 10 percent when they were considered separately. The two townships comprise 19,000 hectares (47,000 acres), about 10 percent of the Ashland District (Figure 3).

TABLE 1. FOREST TYPE AREA ESTIMATES FOR SAMPLE TOWNSHIPS FROM SEVEN ISLANDS LAND COMPANY AND LANDSAT INVENTORIES.*

Forest Type	7 Islands Tally (ha)	Landsat Tally (ha)	Percent Diff.
Sample Township #1			
Softwood	4 331	4 573	+5.6%
Mixed Wood	3 320	3 117	−6.1%
Hardwood	830	906	+9.2%
Total For.	8 481	8 596	+1.4%
Sample Township #2			
Softwood	4 247	4 017	−5.4%
Mixed Wood	3 286	3 591	+9.3%
Hardwood	1 826	1 667	−8.8%
Total For.	9 360	9 275	−0.9%
Sample Townships #1 and #2 Combined			
Softwood	8 578	8 591	+0.2%
Mixed Wood	6 606	6 707	+1.5%
Hardwood	2 656	2 572	−3.2%
Total For.	17 840	17 870	+0.2%

* Both Seven Islands and Landsat tallies were normalized so that total area in each township matched the deeded acreage as listed in the Seven Islands records.

Boundaries of the management units (townships) were superimposed on the Landsat data using a masking program. They were taken from topographic maps, using water bodies as control points.

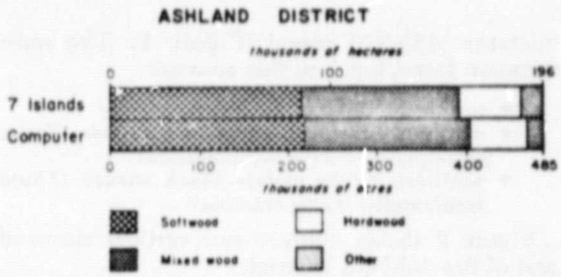

FIG. 4. Seven Islands Land Company inventory tallies for the Ashland District and Landsat computer classification results for the same area.

RESULTS

RESULTS RELATIVE TO THE GOALS

Map the District. A printout map and acreage tally by category was made for each management unit in the Ashland District.

Match Seven Islands categories. Area comparison is one measure of how well the Landsat categories match Seven Islands categories. Area tallies for the entire district are shown in Table 2 and Figure 4. Differences between Landsat and Seven Islands forest type acreage estimates are under 5 percent. As is to be expected, they are larger for the individual township tallies. Figure 5 shows Seven Islands versus Landsat acreage estimates for the individual townships for softwood, mixed wood, hardwood, total forest, water, and open categories. Both the Landsat and the Seven Islands inventory acreage tallies were normalized so that the total acreage in each township matched

TABLE 2. AREA ESTIMATES OF FOREST TYPES AND RELATED FEATURES IN THE ASHLAND, MAINE DISTRICT DERIVED FROM SEVEN ISLANDS LAND COMPANY INVENTORY AND LANDSAT COMPUTER CLASSIFICATION.

	Seven Islands		Landsat		Difference	
	Hectares Acres	% of Total	Hectares Acres	% of Total	Hectares Acres	%
Softwood	87 104	44.4%	88 884	45.3%	+1 780	+ 2.0%
	215 285		219 683		+4 398	
Mixed Wood	71 976	36.7	74 498	37.9	+2 522	+ 3.5
	177 895		184 127		+6 232	
Hardwood	27 482	14.0	26 121	13.3	−1 361	− 5.0
	67 924		64 561		−3 363	
Water	5 911	3.0	4 695	2.4	−1 216	−20.6
	14 609		11 605		−3 004	
Open Land	823	0.4	663	0.3	− 160	−19.5
	2 035		1 639		− 396	
Bog	3 060	1.6	242	0.1	−2 818	−92.1
	7 562		599		−6 963	
Unclassified*	......	......	1 255	0.6	......	......
	......		3 102		......	
Total Forest	186 562	95.0	189 503	96.5	+2 941	+ 1.6
	461 104		468 371		+7 267	
Total Area**	196 356	100.0	196 356	100.0	......	......
	485 310		485 310		......	

* The Seven Islands inventory included no "unclassified" category.
** Both Seven Islands and Landsat tallies were normalized so that total area in each township matched the deeded acreage as listed in the Seven Islands records.

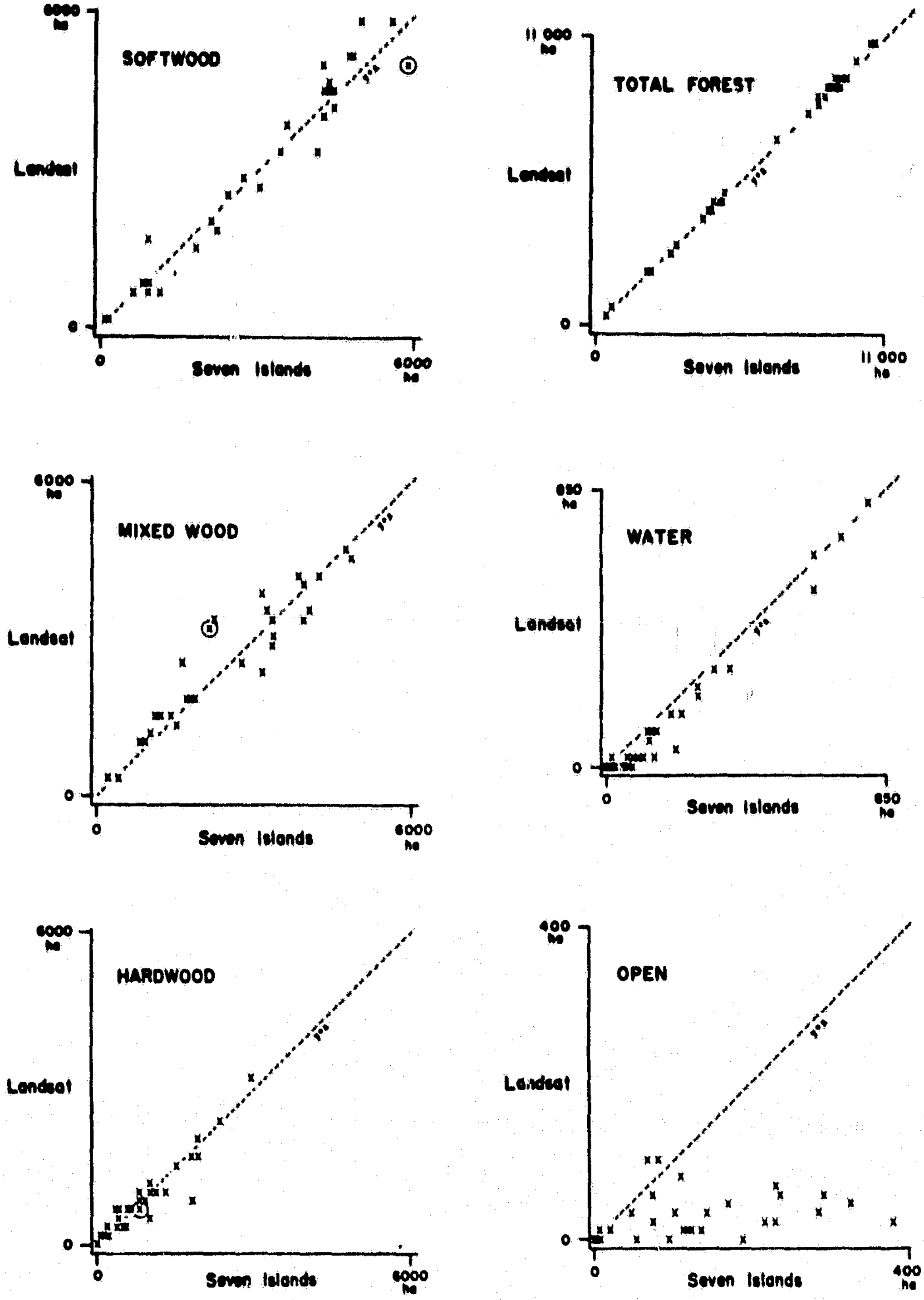

FIG. 5. Seven Islands inventory tallies for each management unit (township) are plotted against Landsat computer classification results for six land cover classes. Discrepancies in one township could be attributed to differences in classification of partially cut areas (data point is circled).

its deeded acreage as listed in the Seven Islands records.

Agreement in locations of features on maps was desired as well as area agreement. An informal comparison of Landsat maps and Seven Islands inventory maps shows that the positions and shapes of the forest stands generally coincide (Figure 6). As a more formal test of locational agreement, 130 sample pixels in one ground truth township were selected at random, and their Landsat and Seven islands categories were compared. Results are in Table 3. The overall agreement (diagonal entries in the table divided by the total number of samples; 83/130) is 63 percent. While this seems rather low, other Landsat applications studies involving forest types have similarly low overall agreement, depending on exactly what the categories are, how they are aggregated, and how the samples are chosen (Table 4). Overall agreement ranges from 43 percent to 98 percent.

This single pixel method of measuring classification accuracy has inherent problems. Minimum feature size classified on the ground truth maps is often greater than one pixel (0.4 hectares or 1.1 acres); in this case it was 4 hectares (10 acres). Exact location of one-pixel samples on ground truth maps is uncertain. Each of these problems can lower the measured accuracy of a classification, regardless of its actual accuracy.

In the non-forest categories, it was found that roads were not located with enough accuracy to be useful; also, bogs were often classified as forest, and small streams were not identified.

Tallies for each township. Acreage by township and category is in Figure 5 as mentioned above. Locating township boundaries was very time consuming but essential for comparison with the standard inventory results.

Geocorrected data. The Landsat geometric correction used was a systematic correction applied to the entire Landsat scene, using a nearest neighbor resampling scheme. The accuracy was acceptable over the one-township size units (8000 hectares or 20,000 acres) used in the Seven Islands project.

REMARKS ON THE CONSTRAINTS

Minimize ground truth. Originally, the Seven Islands inventory of the two sample townships

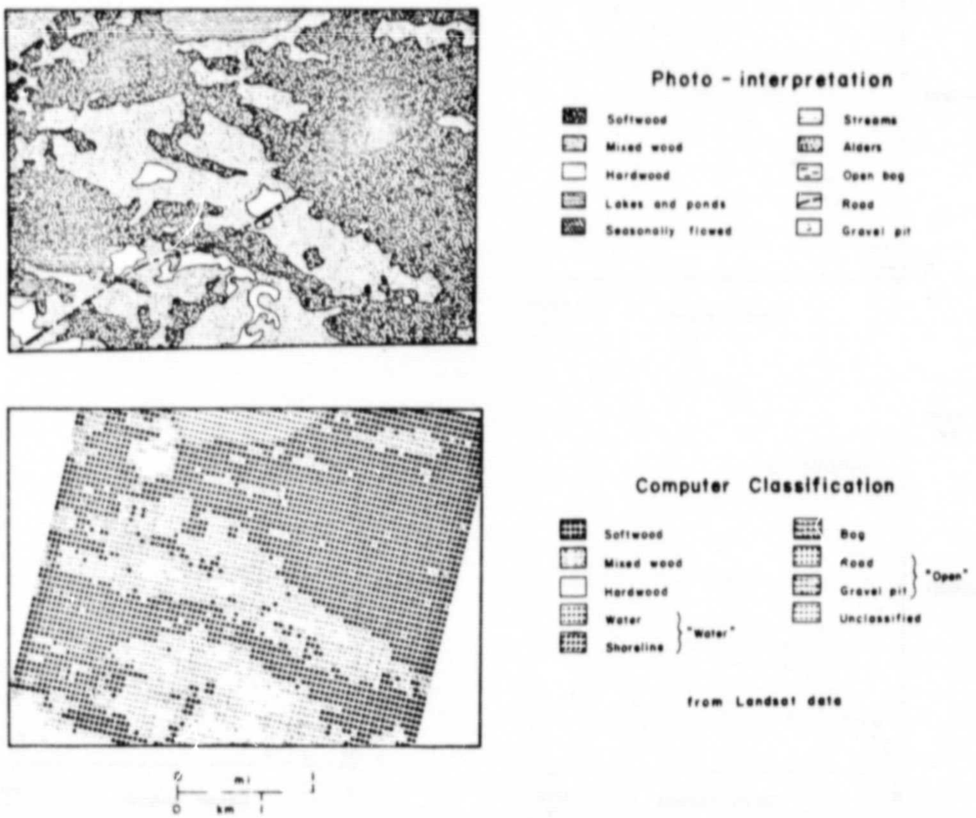

FIG. 6. Seven Islands inventory map (above) and Landsat computer classification (below) from one of the two sample townships. Informal comparison shows that positions and shapes of forest stands generally coincide. Landsat data has been systematically geometrically corrected (original scale 1:24,00).

TABLE 3. COMPARISON OF SEVEN ISLANDS AND LANDSAT CLASSIFICATIONS. THE 130 ONE-PIXEL SAMPLES WERE SELECTED AT RANDOM FROM ONE SAMPLE TOWNSHIP.

Landsat Category	Seven Islands Categories						
	Soft	Mixed	Hard	Water	Open	Other	Total
Softwood	41	12	1	1	0	3	58
Mixed Wood	16	23	3	0	0	2	44
Hardwood	0	8	6	0	0	1	15
Water	0	0	0	12	0	0	12
Open	0	0	0	0	0	0	0
Other	0	0	1	0	0	0	1
Total	57	43	11	13	0	6	130

Sum of diagonal entries = 82, or 63% of the 130 samples total.

was not included in ground truth. Preliminary results, however, showed a large discrepancy between Landsat and inventory maps. The only way to match given categories was to have a sample of them, not just the inventory specifications. Since the size of the ground truth sample townships was large, the original goal was expanded from mapping three townships to mapping the entire district.

Costs. The cost estimates for this project are listed in Table 5. The overall cost of 6.5 cents per hectare (2.6 cents per acre) includes human time at ten dollars per hour, computer time at 600 dollars per hour (on an IBM 360/95), and ground truth. The cost of ground truth for the two sample townships is 37 percent of the total cost—2.4 cents per hectare (0.99 cents per acre). The cost also reflects inefficiencies which would be eliminated in subsequent projects. The estimate excludes cost of software development, depreciation on the computer, photo-mosaics, topographic maps, and geocorrection of data. Classification of a larger area would reduce the per area cost; estimated cost for 800,000 hectares (2 million acres) is 2.4 cents per hectare (0.96 cents per acre). Table 6 compares this cost estimate with those from other Landsat applications projects. They vary from 0.078 to 8.6 cents per hectare (0.032 to 3.5 cents per acre). Much of this variation is due to differences in the items included in the estimates (sometimes ground truth is excluded) and the cost assigned to the items (cost of human time varies from 5 to 21 dollars per hour).

The information derived by computer-classification of Landsat data could also be derived from standard photo-interpretation techniques. The company that did the Seven Islands inventory gave a ball-park estimate of the cost as 11.0 to 16.0 cents per hectare (4.5 to 6.5 cents per acre). (Rate for the Seven Islands inventory itself would be higher because it is more detailed).

DISCUSSION

Although acreage results on the forest categories were within 5 percent, those for the remaining categories (water, bog, open land) had much larger discrepancies (Table 2; Figure 5). Possible explanations of these discrepancies follow. First, there is a smaller sample: together the open, bog, and water categories comprise only 5 percent of the

TABLE 4. COMPARISON OF LOCATIONAL AGREEMENT RESULTS.

Reference	# Categories	# Diagonal Entries (Pixels)	Total # of Samples (Pixels)	Overall Agreement (Percent)	Sample Selection Scheme
Bryant *et al.*	6	82	130	63%	Random
Harding and Scott 1978	5	142	302	47%	Stratified
Johnson *et al.* 1979	6	107	200	54%	Grid
Johnson *et al.* 1979	3	169	200	85%	Grid
Kalensky and Scherk 1975	4	1119	1342	83% (4-date)	*
Kalensky and Scherk 1975	4	*	*	67%-82% (1-date)	*
Kalensky *et al.* 1979	9	4024	4123	98%	Control Areas
Kalensky *et al.* 1979	9	4061	4123	98%	Control Areas
Kalensky *et al.* 1979	9	3978	4123	96%	Control Areas
Kirby *et al.* 1975	6	401	676	59%	Pixel Columns
Mead and Meyer 1977	11	560	1305	43%	Pixel Rows
Mead and Meyer 1977	11	779	1478	53%	Pixel Rows
Williams and Haver 1976	6	162	232	70%	Random
Williams and Haver 1976	3	208	232	90%	Random

* Information not provided.

TABLE 5. SEVEN ISLANDS PROJECT COST ESTIMATES.
SIZE OF AREA CLASSIFIED: 196 400 HECTARES (485 310 ACRES).

Item	Cost (Dollars)	% of Total	Cost/ha (Cents)	Cost/a (Cents)
Materials[1]	$ 699	5.4%	0.36¢	0.14¢
Field Expenses[2]	780	6.1	0.40	0.16
Inventory of Sample Townships[3]	4 800	37	2.4	0.99
Signature Development[4]	4 490	35	2.3	0.93
Subtotal: Initial Costs	$10 769	84 %	5.5 ¢	2.2 ¢
Run-off and Tally of Ashland District[5]	$ 2 070	16 %	1.1 ¢	0.43¢
Total Cost	$12 839	100 %	6.5 ¢	2.6 ¢
Projected Cost Estimate for 800 000 hectares (2 000 000 acres)				
Initial Costs (As Above)	$10 769	56 %	1.3 ¢	0.54¢
Run-off and Tally	8 600	44	1.1	0.43
Total Cost	$19 369	100 %	2.4 ¢	0.97¢

[1] Includes air photos, Landsat images, Landsat CCT's, and computer supplies.
[2] Includes travel and labor costs. (Labor valued at $10 per hour.)
[3] Estimated cost for 19 500 hectares (48 000 acres) at 25¢ per hectare (10¢ per acre).
[4] Includes 305 hours labor and 144 minutes computer time (valued at $10 per minute).
[5] Includes 106 hours labor and 90 minutes computer time.

area classified; the rest is forested. Next, the resolution of Landsat (80 metres) is coarse relative to streams and narrow roads. These features are absorbed into the surrounding forest types. This may account for the Landsat underestimation of water and open categories.

Confusion in Landsat categories may account for the underestimation of the bog category. Bogs were often classified as mixed wood or hardwood.

Forest acreage tallies for some individual townships had noticeably large discrepancies. In one case (circled in Figure 5) this could be attributed to difference in classification of partially cut areas which included many small softwood trees and a few large hardwood trees. The photo-interpretation in the Seven Islands inventory, which is based on numbers of trees, indicated softwood; the computer classification, based on average reflection, indicated mixed wood.

A factor influencing forest classification is sun illumination. Classifications of forest areas within terrain shadows have a bias toward softwood. Merging of digital topographic data and Landsat data could improve this situation (Krebs and Hoffer, 1976; Strahler *et al.*, 1979). Over a large enough area, these differences balance each other out.

There are some problems which researchers cannot solve. One is New England weather, which is relatively cloudy. It is possible that in some years there would be no Landsat coverage at the desired times of year. Another problem is the acquisition of data. At this point there is a long turn-around time in ordering Landsat computer compatible tapes (CCT's). Also some private organizations do not want to depend on government sources for their data.

CONCLUSION

Bearing in mind the objective to give quick, inexpensive, and accurate acreage estimates of forest types to the Bureau of Taxation, the following conclusions are drawn. Results were very good on the district as a whole, but were not good for the individual townships. Each township has unique records of accounting and ownership and must have proven and precise forest type information. In some cases this is needed for portions of a township that are as small as 400 hectares (1000 acres). The 400 hectare tract requires the same level of precision that was reached in this project with the tallies for the 200,000 hectare tract.

On the other hand, the energy situation is becoming more burdensome, and satellite information will become more important as a supplement to aerial photographs and other information sources. Further research in satellite data processing techniques could bring the information to a more useable level and is worth pursuing.

RECOMMENDATIONS

More experience using satellite data in practical situations is recommended. Computer classification may currently be as reliable as photo-

TABLE 6. COST ESTIMATE COMPARISON.

Reference	Items Included: Lndst Data	Items Included: Geocor. of Data	Items Included: Grnd Trth	Items Included: Computer Time	Items Included: Computer Depreciatn.	Value of Human Time ($/hr)	Related to Other Maps?	Size of Subunits 1 000ha	Size of Subunits 1 000a	Total Area Classified 1 000ha	Total Area Classified 1 000a	Total Cost ($)	Cost per ha (¢)	Cost per a. (¢)
Bryant *et al.*	yes	no	yes	yes	no	$10	15' USGS	6.8	16.7	196	465	$12 839	6.5 ¢	2.6 ¢
Gaydos, 1978	yes	yes	no	yes	a/	7	1:250 000	1 700	4 200	560	1 400	442	0.078	0.032
Hill-Rowley & Enslin, 1979	a/	a/	a/	yes	a/	a/	1:250 000	1 700	4 200	2 300	5 600	5 420	0.24	0.097
Kalensky *et al.*, 1979	no	yes	a/	yes	yes	22	UTM	10	25	250	617	21 512	8.6	3.5
Krebs and Hoffer, 1976	no	yes	no	yes	a/	5	7.5' USGS	58	144	464	1 148	2 900	0.63	0.25
Krebs and Hoffer*	a/	yes	yes	yes	a/	5	7.5' USGS	58	144	464	1 148	17 907	3.9	1.6
Roberts and Merritt, 1977	yes	a/	no	yes	no	a/	a/	50	123	50	123	400	0.80	0.32
Williams and Haver, 1976	yes	a/	no	yes	a/	0	7.5' USGS	58	144	263	650	2 250	0.86	0.34

* Includes merging Landsat data with digital topographic data and manual analysis of imagery.
a/ Information not provided.

interpretation, but there are differences, and they need to be identified. Perhaps some of the information missing in the current Landsat maps can be extracted from higher resolution data such as the quarter acre resolution projected for Landsat D (Williams and Stauffer, 1979). Already, examination of Landsat 3 RBV imagery suggests that woods roads will be much more distinct with 30 metre resolution.

SUMMARY

Landsat classification maps were made for a forested area in northern Maine, managed by the Seven Islands Land Company. Over the 200,000 hectare (half million acre) district, results agreed with a standard inventory to within 5 percent on area of general forest types. Cost was estimated at 6.5 cents per hectare (2.6 cents per acre). Accuracy measurements and cost estimates were comparable with other Landsat forestry applications projects.

The techniques described here are promising, but are not yet practical for Seven Islands Land Company's needs. Further research and perhaps better spatial resolution are needed to ensure reliable Landsat results on smaller geographic areas.

ACKNOWLEDGMENTS

This project was supported by NASA Science Grant 5014. We wish to thank Seven Islands Land Company for their cooperation and for the use of inventory data.

REFERENCES

Bauer, Marvin E., Marilyn M. Hixson, Barbara J. Davis, and Jeanne B. Etheridge, 1978. Area Estimation of Crops by Digital Analysis of Landsat Data, *Photogrammetric Engineering and Remote Sensing*, 44(8):1033-1043.

Beaubien, Jean, 1979. Forest Type Mapping From Landsat Digital Data, *Photogrammetric Engineering and Remote Sensing*, 45(8):1135-1144.

Dejace, J., J. Mégier, and W. Mehl, 1977. Computer-Aided Classification for Remote Sensing in Agriculture and Forestry in Northern Italy, *Proceedings of the Eleventh International Symposium on Remote Sensing of Environment*, 2:1269-1278.

Dodge, Arthur G., Jr., and Emily S. Bryant, 1976. Forest Type Mapping With Satellite Data, *Journal of Forestry*, 74(8):526-531.

Gaydos, Leonard, and Willard L. Newland, 1978. Inventory of Land Use and Land Cover of the Puget Sound Region Using Landsat Data, *Jour. Research U.S. Geol. Survey*, 6(6):807-814.

Gaydos, Leonard, 1978. Low-Cost Computer Classification of Land Cover in the Portland Area, Oregon, by Signature Extension Techniques, *Jour. Research U.S. Geol. Survey*, 6(6):815-819.

George, T. H., W. J. Stringer, and J. N. Baldridge, 1977. Reindeer Range Inventory in Western Alaska from Computer-Aided Digital Classification of

Landsat Data, *Proceedings of the Eleventh International Symposium on Remote Sensing of Environment*, 1:671-682.

Harding, Roger A., and Robert B. Scott, 1978. *Forest Inventory with Landsat, Phase II*, Washington Forest Productivity Study, State of Washington Department of Natural Resources, Olympia, WA 98504. 221 p.

Hill-Rowley, Richard, and William R. Enslin, 1979. An Evaluation of Michigan Land Cover/Use Inventories Derived from Remote Sensing: Characteristics and Costs, *Proceedings of the Thirteenth International Symposium on Remote Sensing of Environment*, 3:1251-1259.

Johnson, Gregg R., Eric W. Barthmaier, Tim W. D. Gregg, and Robert E. Aulds, 1979. Forest Stand Classification in Western Washington Using Landsat and Computer-Based Resource Data, *Proceedings of the Thirteenth International Symposium on Remote Sensing of Environment*, 3:1681-1696.

Kalensky, Z., and L. R. Scherk, 1975. Accuracy of Forest Type Mapping from Landsat Computer Compatible Tapes, *Proceedings of the Tenth International Symposium on Remote Sensing of Environment*, 2:1159-1167.

Kalensky, Z. D., W. C. Moore, G. A. Campbell, D. A. Wilson, and A. J. Scott, 1979. Forest Statistics by ARIES Classification of Landsat Multispectral Images in Northern Canada, *Proceedings of the Thirteenth International Symposium on Remote Sensing of Environment*, 2:789-811.

Kirby, C. L., D. Goodenough, D. Day, and P. Van Eck, 1975. Landsat Imagery for Banff and Jasper National Parks Inventory and Management, *Proceedings of the Third Canadian Symposium on Remote Sensing*, Edmonton, Alberta, pp. 207-225.

Kourtz, P. H., 1977. An Application of Landsat Digital Technology to Forest Fire Fuel Type Mapping, *Proceedings of the Eleventh International Symposium on Remote Sensing of Environment*, 2:1111-1115.

Krebs, Paula V., and Roger M. Hoffer, 1976. *Multiple Resource Evaluation of Region 2 U.S. Forest Service Lands Utilizing Landsat MSS Data*, Final Report—Type III. Prepared for NASA/Goddard Space Flight Center, Greenbelt, MD. Institute of Arctic and Alpine Research, University of Colorado; Laboratory for Applications of Remote Sensing, Purdue University; Region 2 U.S. Forest Service, U.S.D.A., 298 p.

Mead, R., and M. Meyer, 1977. *Landsat Digital Data Application to Forest Vegetation and Land-Use Classification in Minnesota*, IAFHE RSL Research Report 77-6, University of Minnesota, St. Paul, Minnesota, 57 p.

Merry, C. J., H. L. McKim, S. Cooper, and S. G. Ungar, 1977. Preliminary Analysis of Water Equivalent/Snow Characteristics Using Landsat Digital Processing Techniques, *Proceedings of the 1977 Eastern Snow Conference*, Belleville, Ontario, Canada, pp. 39-54.

Mukai, Yukio, and Shoji Takeuchi, 1979. Estimation of Primary Production of Vegetation in Agricultural and Forested Areas Using Landsat Data, *Proceedings of the Thirteenth International Symposium on Remote Sensing of Environment*, 2:1177-1188.

Odenyo, Victor A. O., and David E. Pettry, 1977. Land-Use Mapping by Machine Processing of Landsat-1 Data, *Photogrammetric Engineering and Remote Sensing*, 43(4):515-524.

Roberts, Edwin H., and Norman E. Merritt, 1977. Computer Aided Inventory of Forestland, pp. 65-82, In *Inventory of Forest Resources (including water) by Multilevel Sampling*, R. C. Aldrich (Principal Investigator), Type III, Final Report to NASA/Goddard Space Flight Center, USDA Forest Service, Rocky Mountain Forest and Range Experiment Center, Fort Collins, CO.

Sayn-Wittgenstein, L., 1977. Remote Sensing and Today's Forestry Issues, *Proceedings of the Eleventh International Symposium on Remote Sensing of Environment*, 1:267-276.

Strahler, Alan H., Thomas L. Logan, and Curtis E. Woodcock, 1979. Forest Classification and Inventory System Using Landsat, Digital Terrain, and Ground Sample Data, *Proceedings of the Thirteenth International Symposium on Remote Sensing of Environment*, 3:1541-1557.

Titus, S., M. Gialdini, and J. Nichols, 1975. A Total Timber Resource Inventory Based Upon Manual and Automated Analysis of Landsat-I and Supporting Aircraft Data Using Stratified Multistage Sampling Techniques, *Proceedings of the Tenth International Symposium on Remote Sensing of Environment*, 2:1093-1099.

Williams, Darrel L., and Gerald F. Haver, 1976. *Forest Land Management by Satellite: Landsat-Derived Information as Input to a Forest Inventory System*, Intralab Project #75-1, NASA/Goddard Space Flight Center, Greenbelt, MD. 36 p.

Williams, Darrel L., and Mark L. Stauffer, 1979. What Can the Forestry Community Expect from Landsat-D Thematic Mapper Data, *Proceedings of the Symposium on Remote Sensing of Natural Resources*, University of Idaho, Moscow, Idaho.

(Received 30 May 1979; revised and accepted 5 June 1980)

RESULTS OF THE SEPTEMBER 22, 1980 RAVE STUDY

OF THE MOUNT ST. HELENS PLUME

Jarvis Moyers
University of Arizona[a]

This paper presents a description of the joint University-NASA research project RAVE (Research on Atmospheric Volcanic Emissions) and preliminary results from a recent Mount St. Helens expedition. The RAVE scientific team consists of scientists from Drexel University, Dartmouth, Michigan Technological Institute, University of Arizona, University of Maryland, and NASA. A Lockheed Orion P-3 four engine turbo-prop aircraft has been outfitted with active and passive instrumentation for monitoring and sampling gases and aerosols in volcanic plumes. The first field study in this project was performed on September 22, 1980 at the Mount St. Helens volcano. Measurements made in this study include remote sensing of SO_2 and aerosol burdens and fluxes; in plume analysis of SO_2, H_2S, NO, NO_2, O_3 and particle size distribution; and the filter collection of aerosols and reactive gases for subsequent laboratory analysis. There was a very successful integration and operation of all onload equipment and experiments. Available results obtained in this are presented and discussed.

[a]*Chemistry Department, Tucson, AZ 85721*

Enclosure 4

ABSTRACT DIGEST

SYMPOSIUM ON

MOUNT ST. HELENS ERUPTION:

ITS ATMOSPHERIC EFFECTS AND POTENTIAL CLIMATIC IMPACT

Washington, D.C.
November 18-19, 1980

Sponsored by: **NASA-Office of Space and Terrestrial Applications**

On behalf of: **U.S. National Climate Program**

Organized by: Institute for Atmospheric Optics and Remote Sensing

Institute for Atmospheric Optics and Remote Sensing,
P.O. BOX P • HAMPTON, VA 23666

IFAORS

Enclosure 5

CONTRIBUTIONS OF CO_2 AND SO_2 TO THE ATMOSPHERE FROM VOLCANIC ACTIVITY AT MOUNT ST. HELENS

D. M. Harris[a], T. J. Casadevall[b], and D. A. Johnston[c]
U.S. Geological Survey

W. I. Rose, Jr., and T. J. Bornhorst
Michigan Technological University[d]

R. E. Stoiber, L. L. Malinconico, and S. N. Williams
Dartmouth College[e]

The resumption of volcanic activity at Mount St. Helens in March 1980 prompted measurements and study of CO_2 and SO_2 emission rates. The objective of these studies is to provide information about the degassing of the subsurface magma body. Although the principal propellant of the explosive eruptions at Mount St. Helens is probably H_2O vapor, emission rates for CO_2 and SO_2 may also be useful indicators of volcanic activity. Significant changes in emission rates for these gases may occur as a result of various factors such as migration of gases from deeper magma, intrusion of magma toward the surface, changes in the concentrations of CO_2 and/or SO_2 in the silicate liquid, changes in the degassing rate of the silicate liquid, and changes in the permeability of the vent. Aside from providing information relevant to eruption mechanisms, the measurements of sustained gas emissions together with the pre-eruption volatile concentrations provide a basis for inferring the presence of a magma body and for estimating the volume of degassed silicate liquid remaining at depth. The total amounts of CO_2 and SO_2 released to the atmosphere by magma degassing during non-eruptive periods at Mount St. Helens can be estimated from the more than 70 measurements of emission rates. One must increase these numbers by the amounts released during explosive eruptions.

[a]*Reston, VA 22092*

[b]*Vancouver, WA 97663*

[c]*Menlo Park, CA 94025 (deceased)*

[d]*Houghton, MI 49931*

[e]*Hanover, NH 03755*

Enclosure 6

SEAN Bull Vol 5 #12 Dec 31, 1980

Extract
SEAN Bulletin #12
Dec 31, 1980

Volcanic Activity
Tarumai Volcano (cont.)

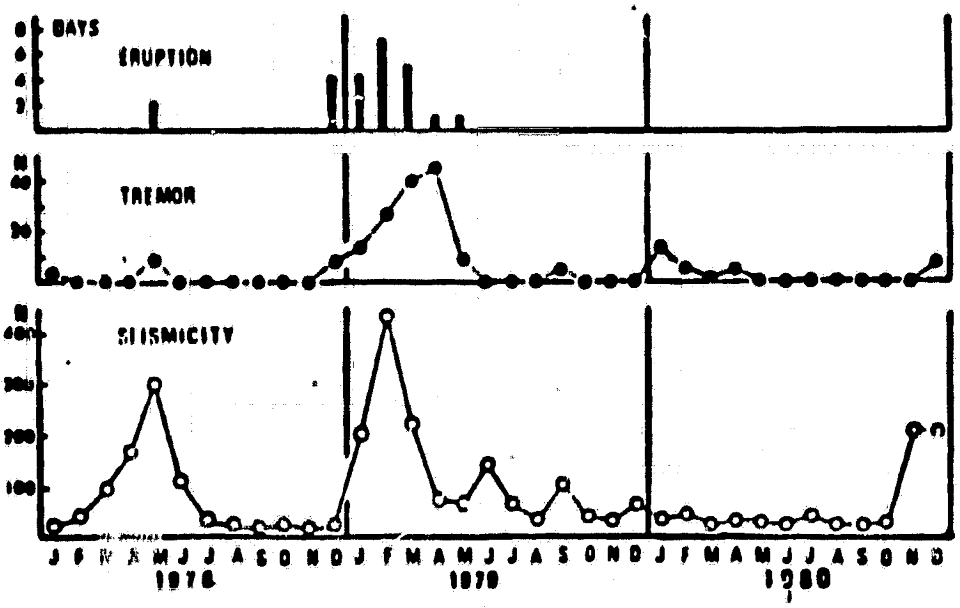

Figure 3: Monthly numbers of days in which eruptions occurred (top); harmonic tremor events (center); and recorded earthquakes (bottom) at Tarumai, January 1978 - December 1980.

Mayon Volcano, SE Luzon Island, Philippines (13.26°N, 123.62°E). All times are local (= GMT + 8 hours).

A moderate quantity of dirty white steam rose weakly to 200 m above the crater rim on 4 December at 1247, accompanied by short-duration harmonic tremor on the Mayon Resthouse Observatory seismograph. Faint crater glow was first noted at 2315 the same day. Additional steam emission was observed 12 and 14 December.

Harmonic tremor was first recorded at Mayon on 16 August (see SEAN Bulletin v.5, no. 8). Episodes of tremor and discrete earthquakes continued through December. Similar seismic activity preceded the 1978 eruption (see SEAN Bulletins v.3, nos. 2, 5, and 8) and accompanied crater glow in July 1979 (see SEAN Bulletin v.4, no. 8).

Information Contact: Olimpio Peña, Acting Commissioner, Commission on Volcanology, 5th Floor, Hizon Bldg., Quezon Blvd. Ext., Quezon City, Philippines.

Volcanic Activity in Nicaragua, El Salvador, and Guatemala, late 1980

Geologists from Dartmouth College, the Instituto Geográfico Nacional of Guatemala, and the Instituto de Investigaciones Sísmicas of Nicaragua observed 8 Nicaraguan, 2 Salvadoran, and 2 Guatemalan volcanoes between mid-November and early December. Dartmouth geologists provided the following report.

Nicaragua

Cerro Negro (12.52°N, 86.73°W) - Summit crater fumaroles remained at temperatures as high as 300°C. A small vapor plume was intermittently visible. Seismic activity had dropped from the high level of June.

Cosiguina (12.97°N, 87.58°W) - No fumarolic activity was visible from the rim.

Enclosure 7

Volcanic Activity
Nicaragua, El Salvador, Guatemala, (cont.)

Las Pilas (El Hoyo) (12.48°N, 86.68°W) - A small continuous vapor plume was still being emitted from the top of the km-long crack in the summit.

Masaya (11.95°N, 86.15W) - Emission of a very large gas plume has continued without interruption since fall, 1979. Remote sensing of SO_2 revealed continued high level flux, with 1,500 - 2,000 tons/day average for the entire year. The hole through the surface of the lava lake was larger than in previous years and a great deal of sublimation was occurring around its edge. No lava or red glow was visible during daylight. Acid gas and rain continued to cause considerable damage downwind.

Mombacho (11.83°N, 85.98°W) - A small, intermittent plume was visible, rising from the SE section of the summit.

Momotombo (12.42°N, 86.55°W) - The summit crater fumaroles continued to be very hot with temperatures measured up to 735°C and reported to >900°C. A small vapor plume continued and remote sensing revealed very low rates of SO_2 emission. Portions of the crater were seen to glow red and orange when observed at night, with the highest temperatures on the steep S wall of the crater. No seismic activity has occurred recently at Momotombo.

San Cristóbal (12.70°N, 87.02°W) - A moderate-sized vapor plume rose continuously from the summit. Remote sensing of SO_2 revealed increased flux since June 1980, but SO_2 emission remained far below the levels of the mid-1970's.

Telica (12.60°N, 86.87°W) - A moderate-sized but continuous vapor plume rose from the summit crater. SO_2 flux was remotely measured and found to be approximately 150 tons/day.

El Salvador

Observations were made during a flight over the country.

Santa Ana (13.85°N, 89.63°W) - A moderate plume rose from a bank of fumaroles on the SE wall of the inner crater, very similar to its appearance in November 1978.

San Miguel (13.44°N, 88.27°W). - A small, continuous vapor plume rose from the summit crater.

Guatemala

Pacaya (14.38°N, 90.60°W) - A very small cinder cone had grown inside MacKenney Crater in the last 2 months. A large gas plume rose continuously from the summit.

Santiaguito (14.76°N, 91.55°W) - Ash and gas eruptions from Caliente vent (at the E end of Santiaguito Dome) occurred irregularly over the 3-day period of observation, with intervals of 1/2 hour to 4 hours between eruptions. Most eruptions lasted 2-3 minutes and sent ash and gas columns to heights of several hundred m to 1 km above the vent. Five mm of ash accumulated at the foot of the dome over one 12-hour period. Eruptions

Volcanic Activity
Nicaragua, El Salvador, Guatemala (cont.)

occasionally threw 10-cm blocks several hundred m and ejected tephra to well above the summit of Santa María. Although not directly observed, the plug dome and blocky lava flow that was seen being extruded from Caliente vent in February was apparently still very active. Large avalanches of glassy material could be heard from Caliente vista many times per hour. Debris from these avalanches was visible in the barranca below Santiaguito.

Information Contacts: Richard E. Stoiber, Stanley N. Williams, H. Richard Naslund, Lawrence L. Malinconico, and Mark Conrad, Department of Earth Sciences, Dartmouth College, Hanover, New Hampshire 03755 USA.

Samuel Bonis, Instituto Geográfico Nacional, Avenida las Américas, 5-76, Zona 13, Guatemala City, Guatemala.

Arturo Aburto and Douglas Fajardo, Instituto de Investigaciones Sísmicas, Apartado Postal 1761, Managua, Nicaragua.

SEISMIC EVENTS

Earthquakes

DATE	TIME (GMT)	MAGNITUDE	LAT.	LONG.	DEPTH OF FOCUS	REGION
7 Dec.	1737	5.7 Ms	36.02°N	1.23°E	10 km	N Algeria
17 Dec.	1622	6.7 Ms	49.41°N	129.61°W	10 km	W of Vancouver Is., Can
19 Dec.	0117	6.1 Ms	34.54°N	50.70°E	Shallow	N-central Iran
22 Dec.	1251	5.5 mb	34.39°N	50.49°E	32 km	N-central Iran

The Algeria event injured 20 persons in the El Asnam area, devastated by earthquakes 10 October that killed thousands and left about 400,000 homeless (see SEAN Bulletin v.5, no. 10). There were no reports of casualties or damage from the 17 December shock. The 19 December earthquake killed 26 persons. The nearby event 3 days later caused 3 deaths and 139 injuries according to official reports.

Information Contacts: National Earthquake Information Service, U.S. Geological Survey, Stop 967, Denver Federal Center, Box 25046, Denver, Colorado 80225 USA.

United Press International.

The Associated Press.

Earthquake Swarm
Siquijor Island, Philippines.

A swarm of earthquakes began to be felt at Lazi, on the S coast of Siquijor Island, on 17 December. By 19 December, recorded events averaged 102/hour and several may have reached magnitude 4-5. Loud detonations reportedly accompanied the seismicity. The next day, 95 strong earthquakes

EOS

TRANSACTIONS AMERICAN GEOPHYSICAL UNION
VOLUME 61 NUMBER 46 NOVEMBER 11, 1980

1980 AGU FALL MEETING

December 10-15, 1980, San Francisco

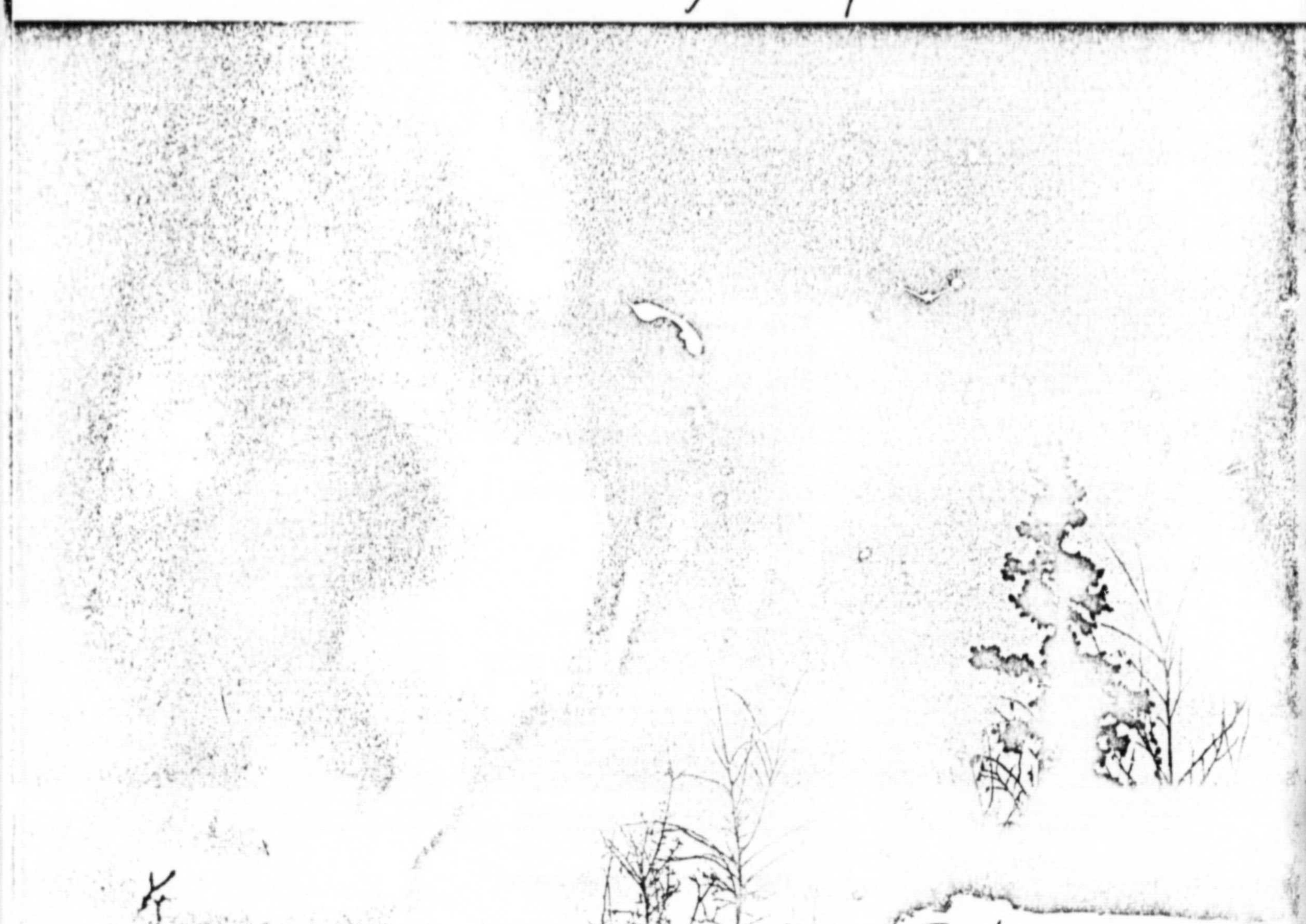

Enclosure 8

rest on a fan of earlier 1980 pyroclastic flow deposits. The paths of the basal portions of the flows were controlled by topography. Billowing, convecting clouds of ash that emanated from the dense, ground-hugging flows probably were produced by elutriation of fine particles from the fluidized mass by escaping gases. That incorporated air may have been an important component of those gases is suggested by temperatures determined on a flowage deposit soon after emplacement, which generally decreased toward the terminus of the flow. This decrease, of more than 200°C, may be due to progressively greater cooling of the flowing mass by incorporated air with increasing distance from the vent. Expansion of air incorporated and heated in the pyroclastic flows could have contributed to the fluid behavior of the flows. One pyroclastic flow observed on August 7 traversed 5.7 km in 7 minutes through an elevation drop of 750 m, attaining a maximum speed of 100 km/hr. Velocities over various segments of the flow path appear to have been controlled by slope angles.

V 35

MT. ST. HELENS LAVA DOME: PETROGRAPHY AND MINERAL CHEMISTRY

L.D. Raedeke, E.A. Mathez and A.J. Irving
(Dept. of Geological Sciences, University of Washington, Seattle, WA 98195)

The Mt. St. Helens lava dome, emplaced shortly after the June 12, 1980 eruption is a porphyritic dacite. Plagioclase (32 modal %) dominates the phenocryst assemblage as .5-2mm euhedral to subhedral laths. Most plagioclase show concentric, nearly continuous zoning from a subhedral core to a euhedral rim. Glass (± fluid) inclusions mottle the cores of some crystals, or occur along distinct growth zones near rims. Orthopyroxene phenocrysts (5%) occur as elongate euhedral prisms (≤1mm). Hornblende (3.5%) forms subhedral crystals which commonly are rimmed by a zone of fine-grained magnetite + pyroxene + glass. Magnetite and ilmenite (0.5%) occur as small phenocrysts or as inclusions in silicates. Clinopyroxene phenocrysts are rare. Neither biotite nor quartz were found. The groundmass (60%) is mostly rhyolitic glass (~75% SiO_2) with abundant microphenocrysts of plagioclase. Electron microprobe analysis of the plagioclase phenocrysts shows that normal zoning is most common, with mean core compositions of An 56 (range An 48-66) and rims of An 50 (range An 44-59). Although rare, some plagioclases were found with strong reverse zoning from cores of An 33 to rims of An 50. Hornblendes (tschermakitic) are also slightly zoned and have two distinct populations: 1) molar Mg/Mg+Fe*=.72, molar K/K+Na=.07 and 2) Mg/Mg+Fe*=.64 K/K+Na=.14. Hypersthene (Wo2En65Fs33) and augite (Wo43En42Fs15) are relatively constant in composition. The oxides are typically Usp33Mt67, and Ilm81Hm19. Using the Buddington and Lindsley (1964) geothermometer and assuming equilibrium, these oxide compositions yield a crystallization T=945°C and $f_{O_2} \sim 10^{-10.4}$. The two distinct chemical populations of plagioclase and hornblende indicate the participation of at least two compositionally distinct magmas in the formation of the June 12 lava dome.

V 36

MT. ST. HELENS LAVA DOME, PYROCLASTIC FLOW AND ASH SAMPLES: MAJOR AND TRACE ELEMENT CHEMISTRY

A.J. Irving (Dept. of Geological Sciences, Univ. of Washington, Seattle, WA 98195)
J.M. Rhodes and J.W. Sparks (Dept. of Geology, Univ. of Massachusetts, Amherst, MA 01003)

Samples of the lava dome emplaced in the crater of Mt. St. Helens several days after the June 12, 1980 eruption, pumice boulders from the May 18, May 25, July 22 and August 7 pyroclastic flows, and various ash samples from different locations have been collected for chemical analysis. Here we present XRF and INAA data for the dome, one pumice boulder and three ash samples. The rock samples and two of the three ash samples are similar in major elements, indicating that the 1980 magma has remained fairly uniform in composition over the period May to August. The magma is a medium-K, SiO_2-poor dacite. The June 12 ash sample has lower SiO_2 and K_2O, and higher Al_2O_3, total FeO, MgO and CaO, and may have experienced airborne enrichment in phenocryst minerals. The rock samples are light-REE enriched with a possible slight positive Eu anomaly, and contain 12-13 ppm Co, 8-13 ppm Cr, 71-100 ppm V, 9-10 ppm Sc and 270-290 ppm Ba.

[illegible]	[illegible]	[illegible]	[illegible]	[illegible]	[illegible]	[illegible]
[illegible]	[illegible]	[illegible]	[illegible]	[illegible]	[illegible]	[illegible]
[illegible]	[illegible]	[illegible]	[illegible]	[illegible]	[illegible]	[illegible]
[illegible]	[illegible]	[illegible]	[illegible]	[illegible]	[illegible]	[illegible]
[illegible]	[illegible]	[illegible]	[illegible]	[illegible]	[illegible]	[illegible]
[illegible]	[illegible]	[illegible]	[illegible]	[illegible]	[illegible]	[illegible]
[illegible]	[illegible]	[illegible]	[illegible]	[illegible]	[illegible]	[illegible]
[illegible]	[illegible]	[illegible]	[illegible]	[illegible]	[illegible]	[illegible]
[illegible]	[illegible]	[illegible]	[illegible]	[illegible]	[illegible]	[illegible]
[illegible]	[illegible]	[illegible]	[illegible]	[illegible]	[illegible]	[illegible]
[illegible]	[illegible]	[illegible]	[illegible]	[illegible]	[illegible]	[illegible]

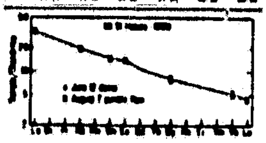

V 37

RHEOLOGICAL PROPERTIES OF MUDFLOWS ASSOCIATED WITH RECENT ERUPTIONS OF MOUNT ST. HELENS

J. Fink
M. Malin (Geology Department, Arizona State University, Tempe, AZ 85281)

Rheological properties of three superposed mudflows on the south side of Mount St. Helens were calculated using techniques based on the geometry of the flow deposits. Measurements of the sizes and densities of suspended blocks, thicknesses and slopes of levees, and inclination of the flow surfaces as they moved around banked curves gave estimates for yield strengths, plastic viscosities, mean flow velocities, and volumetric flow rates. The lowermost flow had the largest volume, smallest median grain size (115μ), lowest yield strength (400 N/m^2), highest mean velocity (31 m/s) and volumetric flow rate (3400 m^3/s). The two later flows (middle; upper) had larger grain sizes (480μ; 600μ) and strengths (1000 N/m^2; 1100 N/m^2) and lower velocities (10 m/s) and flow rates (300 m^3/s). An upper bound of 300 $N\text{-}s/m^2$ was placed on plastic viscosity of the lowermost flow; estimates for the upper flows could not be obtained. The lowermost flow was probably caused by the catastrophic eruption of May 18, when large volumes of ice and rock were mobilized. Later smaller mudflows were observed forming by failure of the snow and ash-covered slopes on the south rim of the mountain in mid-June.

Yield strength measurements are being used in conjunction with rainfall, topographic and ash thickness data to predict areas of highest susceptibility to new mudflow formation during the upcoming rainy season.

The 1980 Eruption of Mt. St. Helens IV

Emerald Room HI
Tuesday PM
Robert L. Christiansen (USGS), *Stephen D. Malone* (U of Washington), Presiding

V 38

EXPLOSIVE VOLCANISM: POSSIBLE SOURCE OF AGGREGATE FORMATION ON MARS

D.W. Krinsley, J. Fink, and R. Greeley (Department of Geology, Arizona State University, Tempe, AZ 85281)

The recent eruptions of Mount St. Helens illustrate the important effects which large volumes of volcanic ejecta may have on the opacity of the atmosphere, which in turn could effect climate. Hence, any process which modifies grain size will strongly influence atmospheric dispersal, as well as effecting subsequent near surface eolian transport.

During the ash fall in Portland, Oregon, which accompanied the June 12 eruption, large particles were observed which broke into smaller grains upon impacting the ground. This suggests that the particles were composed of smaller ones, loosely bonded. These so called "aggregates," have been used to explain several eolian phenomena on Mars. Theory, observations and laboratory experiments suggest that the sand-sized fraction on Mars is depleted. However, it is generally accepted that sand-sized particles are necessary for the formation of dunes on Mars. A proposed solution is the creation of electrostatically bonded aggregates by mechanical abrasion; these have been produced in the laboratory.

Aggregate formation has been attributed exclusively to eolian abrasion; however, the mechanical disintegration required to produce aggregates also occurs during explosive volcanic eruptions. Recent observations from Mount St. Helens suggest that eruptions may indeed produce electrostatic aggregates, although their formation may be hindered by atmospheric water. Volcanically derived aggregates dispersed by global winds could significantly increase the population of sand sized particles to the level necessary to form extensive dune fields on Mars. Large concentrations of fine grained, unconsolidated materials near Martian volcanoes could be made of sand sized aggregates, rather than smaller ash particles.

V 39 INVITED PAPER

VARIATIONS OF SO_2 AND CO_2 EMISSION RATES AT MOUNT ST. HELENS, MARCH 29 TO JULY 22, 1980

T. J. Casadevall, D. Johnston, D. M. Harris
(U. S. Geological Survey, Vancouver, WA 98660)
R. E. Stoiber, S. N. Williams, and
L. L. Malinconico (Dartmouth College, Hanover, NH 03755)

The objective of these studies is to provide information about the degassing of the subsurface magma body at Mt. St. Helens. Emission rates of SO_2 were determined by ground-based and airborne correlation spectrometry of SO_2 in plumes. Emission rates for CO_2 were determined by measuring CO_2 anomalies along flight paths normal to the plume trajectory at various altitudes, the cross sectional area of the plume, and the wind velocity. SO_2 measurements began on March 29 and CO_2 on July 6.

From March 29 to May 14 SO_2 emission rates were between 10 and 50 metric tons/day (Td^{-1}) No additional SO_2 emission data was obtained until the afternoon of the May 25 eruption, when the rate was 2400 Td^{-1} during light emission of ash. Later, the rate decreased to about 150 Td^{-1} in the absence of ash emission. An increase in SO_2 emission to 1000 Td^{-1} occurred about 7 days before the June 12 eruption and emplacement of the lava dome. The emission rate remained at 1000 Td^{-1} through June 22. On or before July 5, the rate increased to about 2600 Td^{-1}; then from July 6 to 18 it decreased gradually to about 1100 Td^{-1}. About 5 hours before the July 22 eruption, but after the onset of premonitory seismicity, a measurement of 1900 Td^{-1} was obtained. Whether this increase in SO_2 preceeded or followed the seismicity is not known. During the period July 6 - 22, measurements of CO_2 showed a decrease from 10,000 Td^{-1} to about 5,000 Td^{-1}. When the SO_2 emission rate increased abruptly on July 22, the CO_2 emission rate remained low. This caused a large decrease in the CO_2/SO_2 ratio; several interpretations are possible.

V 40 INVITED PAPER

CO_2 EMISSION RATES AT MOUNT ST. HELENS BY AIRBORNE PLUME MEASUREMENTS

D. M. Harris (U. S. Geological Survey, 959 National Center, Reston, VA 22092)
M. Sato (same address)

An airborne method for determining the CO_2 emission rate at Mt. St. Helens was developed because the rate is difficult to obtain from measurements at fumaroles in the crater. The CO_2 concentration variations along flight paths are obtained by an infrared method using continuous flow of air through a 6.75 m pathlength gas cell and transmission measurements at the 4.26 μm absorption band for CO_2. Data from each flight path are corrected for pressure and temperature by using the National Advisory Committee for Aeronautics (NACA) standard atmosphere. Measurements of the CO_2 concentration along flight paths perpendicular to the plume trajectory at various altitudes yield a set of concentration profiles. The mass rate of emission is calculated from the spatially

V 126

FERRIC-FERROUS EQUILIBRIUM IN SILICATE LIQUIDS AT 1 BAR

R.O. Sack (Dept. of Geology & Geophysics, University of California, Berkeley, Ca. 94720)
I.S.E. Carmichael

The concentration of Fe_2O_3 and FeO has been determined in 57 silicate liquids, covering virtually the whole natural range of lavas, quenched from superliquidus temperatures (1200-1330°C) and with ambient oxygen fugacities close to FMQ. In conjunction with published data, the ferric-ferrous ratio in 143 multicomponent silicate liquids is best fitted by an empirical equation relating the natural log of oxygen fugacity, absolute temperature and the composition of the liquid as follows:

$$\ln (X^{liq}_{Fe_2O_3}/X^{liq}_{FeO}) = 0.21813 \ln f_{O_2} + 13184.8/T$$
$$-4.49933 + 2.15036X_{SiO_2}$$
$$-8.35163X_{Al_2O_3} - 4.49507X_{FeO}$$
$$-5.43639X_{MgO} + 0.07311X_{CaO}$$
$$+3.54148X_{Na_2O} + 4.18688X_{K_2O}$$

where X_{FeO} refers to total iron calculated as FeO. Oxygen fugacities calculated for the analysed samples of the Makaopuhi lava lake are systematically low by 0.4 to 1 $\log_{10} f_{O_2}$ depending on temperature, but the correspondence with values derived from coexisting Fe-Ti oxides in fresh andesites and siliceous obsidians is good. The higher oxidation state of alkali-rich basic lavas indicates higher oxygen fugacities (at the same temp.) than is typical of tholeiitic lavas; these necessitate more magnesian olivines to counteract both oxygen fugacity and lower silica activity, in comparison to their tholeiitic counterparts.

V 127

ACCURATE FIRST PRINCIPLES ISOTHERMS FOR NaCl TO 300 KILOBARS

M.S.T. Bukowinski (Dept. of Geology and Geophysics, University of California, Berkeley, Ca. 94720)

Decker's equation of state for NaCl, frequently used for pressure calibration, has satisfactory accuracy to pressures of the order of 150 kilobars. We report an attempt to generate accurate theoretical isotherms for NaCl that are reliable to 300 kilobars.

The 0°K isotherm of NaCl is computed with the aid of a first principles calculation of the energy spectrum and charge density in the B1 structure. The Augmented Plane Wave method was used to obtain the self-consistent band structure. The exchange and correlation interactions were approximated by the Hedin-Lundquist potential, which contains no adjustable parameters. A modified version of the Virial theorem was used to compute the pressure.

The predicted 0°K lattice constant of NaCl is in very good agreement with the best available estimates, as are the zero pressure bulk-modulus and its pressure derivative. Since the accuracy of the theoretical methods improves with compression, we feel that we have a very accurate 0°K isotherm.

Finite temperature isotherms are being generated with the help of available thermodynamic data, including the temperature dependent Gruneisen parameter. Room temperature results will be compared with Decker's equation and available static compression results.

V 128

DISSOLUTION KINETICS OF SELECTED SILICATE MINERALS UNDER ACID CONDITIONS

D. I. Siegel (U.S. Geological Survey, St. Paul, Minn. 55101)

The dissolution of bytownite, microcline, enstatite, augite, biotite, and forsterite in acidified deionized water was investigated at near standard temperature and pressure and constant pH of 4.00 to determine the kinetics of the release of silica, calcium, and magnesium. Release of cations and silica followed parabolic rate laws for about the first 700 hours of reaction time, then linear rate laws from about 700 to 1,800 hours of reaction time. Estimated linear-rate constants for release of silica ranged from $10^{-13.3}$ moles per square centimeter per second for forsterite to $10^{-13.9}$ moles per square centimeter per second for enstatite. Linear-rate constants for release of magnesium ranged from $10^{-14.5}$ to $10^{-16.3}$ moles per centimeter squared per second for forsterite and biotite, respectively. Calcium was released at linear rates ranging from $10^{-14.8}$ to $10^{-16.9}$ moles per centimeter squared per second for augite and microcline, respectively. Release of magnesium from forsterite was about 25 times faster than the release of calcium from bytownite, and was at least two times faster than the release of magnesium from other ferromagnesian minerals. The rate of calcium release from augite was about 10 times faster than calcium release from bytownite. The difference in silica release from plagioclase and forsterite and the much greater rate of magnesium release from forsterite compared to the calcium release from bytownite suggest that (1) chemical weathering of gabbroic rocks in open, acidic systems is generally dominated by the dissolution of olivine and feldspar, and (2) olivine probably weathers at least an order of magnitude faster than feldspar.

V 129

THE PARTITIONING OF REE'S, Sc, Rb and Cs BETWEEN A SILICIC MELT AND A Cl FLUID

E.A. Webster
J.R. Holloway (both at: Geology Department, Arizona State University, Tempe, AZ 85281)

The partitioning of Sm, Eu, Tb, Yb, Lu, Sc, Rb, and Cs between a Si rich melt (79 wt % SiO_2) and an aqueous Cl fluid (.8 molal Cl) has been experimentally determined. Runs were conducted for 10 days at 4 kb and 1000°C in an internally heated argon media pressure vessel. Pt capsules were used. The starting materials were a synthetic Fe-free analogue of the Bishop Tuff and a KCl-$NaCl$-H_2O solution. A vapor to melt ratio of ~ 4:1 was used (200 mg fluid to 50 mg glass). Reversals were obtained by running duplicate capsules with the trace elements initially in either the fluid or in the glass. Relative to the original glass mass, approximate concentrations of 50 ppm for the REE's, 12 ppm Sc, 100 ppm Cs and 250 ppm Rb were used. Trace element concentrations in the starting glass, final glass and vapor solute were determined by INAA.

This Cl fluid does not cause any fractionation between the REE's but does fractionate alkali elements from the REE's. Distribution values (D_i) in mass units are shown below. Mass partition coefficients as concentration in melt/concentration in fluid (including H_2O) can be obtained by multiplying the D_i values by 9.07 ± 1.15 for all elements but Sc and by 9.46 ± .46 for Sc. The uncertainty is chiefly due to incomplete solute recovery.

element	D_i = concentration in glass / concentration in solute
Sc	9.34 ± .45
Rb	.285 ± .042
Cs	.248 ± .030
Sm	9.47 ± .51
Eu	7.60 ± .60
Tb	10.09 ± .70
Yb	10.74 ± .58
Lu	9.24 ± 1.75

V 130

THE COORDINATION CHEMISTRY OF SOME TRANSITION METAL IONS IN HYDROTHERMAL SOLUTIONS

Nicholas J. Susak (Department of Geological and Geophysical Sciences, Princeton University, Princeton, NJ 08544)
David A. Crerar
(Sponsor: W. Jason Morgan)

The visible and near-infrared spectra of Co(II) and Ni(II) have been measured along the liquid-vapor curve of 0-5 m NaCl solutions up to 300°C. At low temperatures and low chloride concentrations (m_{Cl}) these ions are octahedrally coordinated by water and chloride. The absorption peaks of the octahedral (O_h) complex undergo a red-shift with increasing temperature or m_{Cl} in response to increased thermal vibrations or the formation of higher chloride complexes. Above a temperature T_x which is a function of the metal ion and m_{Cl} the O_h complex gradually converts to a tetrahedral complex (T_d) until a temperature T_y above which only the T_d complex is present. The spectra of Fe(II) and Cu(II) up to 90°C show only a red-shifted O_h complex but ligand-field considerations suggest that these ions should also convert to a T_d complex at higher temperatures.

A change to a T_d complex will increase the free energies of the complexed ion thereby changing the equilibrium constants for mineral solvation reactions. This results in higher mineral solubilities. Such stereochemical transformations may account for changes in mineral zoning patterns and may be important as a depositional mechanism.

V 131

HYDROTHERMAL CLAY MINERAL FORMATION OF EAST PACIFIC RISE AND BAUER BASIN SEDIMENTS

Gary M. McMurtry
Hsueh-wen Yeh (both at: Hawaii Institute of Geophysics, Univ. of Hawaii, Honolulu, HI 96822)

Samples of surface metalliferous sediment recovered from the crest of the East Pacific Rise at 6°N and 10°S latitude and from the adjacent Bauer Basin are characterized by authigenically formed, iron-rich montmorillonite that dominates the non-carbonate mineralogy of the clay fraction (<2 µm). Although previous work has suggested that these iron-rich montmorillonites are formed by seafloor-temperature, diagenetic processes, we have obtained oxygen isotopic formation temperatures which indicate that the iron montmorillonites are created by low-temperature (30° to 50°C) hydrothermal processes.

The clay fraction was chemically treated to remove calcium carbonate and iron oxide phases. These treatments did not remove opaline silica phases, which SEM results indicate are largely biogenic in origin. Because biogenic silica phases are ^{18}O enriched, minimum formation temperatures ranging from 2° to 32°C were calculated for the montmorillonite. Maximum formation temperatures ranging from 35° to 56°C were calculated by employing published $\delta^{18}O$ values for biogenic silica in mass-balance equations.

These iron montmorillonites are possibly formed as a result of the cooling and oxidation of unstable, high-temperature (380° ± 30°C) sulfide assemblages recently discovered on the crest of the East Pacific Rise or as a result of the percolation of hydrothermally altered seawater solutions through underlying basalt and sediments. The widespread sedimentation of the clay mineral is suggested to be caused by colloidal transport, possibly by the bottom current erosion of hydrothermal mounds. Hydrothermal iron montmorillonite-nontronite formation may act as a direct and significant oceanic sink for Si and Fe released by the high-temperature alteration of basalt at ocean spreading centers.

Airborne Sampling of Eruption Clouds of Explosive Volcanoes

Gold Rush B
Friday AM
R. D. Cadle, W. I. Rose, Jr. (Michigan Tech.), Presiding

V 132 INVITED PAPER

LONG TERM MONITORING OF SO_2 FLUX AT VOLCANOES

Lawrence L. Malinconico
Richard E. Stoiber (both at: Dept. of Earth Sciences, Dartmouth College, Hanover, NH 03755)

Monitoring SO_2 from several active volcanoes has been carried out with a correlation spectrometer (COSPEC) irregularly for various time intervals over the last eight years. At Fuego and Pacaya, Guatemala and San Cristobal, Nicaragua and to a less marked degree at others we note a slow rise and fall in SO_2 flux over periods of months or years resulting in a change of between one and two orders of magnitude. The maximum is often coincident with periods of increased eruptive activity, either lava or pyroclastic, though not always a major eruption. When these occur, the flux increases to even greater levels. The nine year crisis at San Cristobal, now apparently over, began in 1971 with the first noticeable gas emission since the 17th Century. It culminated with very minor ash eruptions in 1976, coincident with the highest SO_2 flux of thousands of metric tons per day. In 1980 the rate has dropped to 70 tons per day. At Masaya Volcano, Nicaragua, we have measured the beginning of a dramatic new trend. SO_2 emission is almost an order of magnitude greater than it was in the 1970's. Similar events have occurred approximately 25, 50 and 75 years ago and lasted from 5 to 10 years. We are continuing to study this event. These gradual changes in SO_2 flux contrast with short term increases in flux of hours or days duration which have preceded ash eruptions at Mt. Etna, Sicily.

V 133 INVITED PAPER

SHAPES AND CONCENTRATIONS OF VOLCANIC PLUMES MONITORED IN CENTRAL AMERICA AND WESTERN UNITED STATES

Richard E. Stoiber
Lawrence L. Malinconico
Stanley N. Williams (all at: Dept. of Earth Sciences, Dartmouth College, Hanover, NH 03755)
W.E. Winner (Dept. of Biological Sciences, Stanford Univ., Stanford, CA 94305)

The correlation spectrometer (COSPEC) and SO_2 detector (Interscan) have been used both car-borne and airborne to measure the rate of production and concentration of SO_2 in volcanic plumes in Nicaragua, Guatemala, and Washington State. A method of flying at successively lower elevations at a distance downwind from an actively degassing volcano has been developed to determine the plume thickness and lateral dimensions. These data are the bases for construction of "ladders" -- three-dimensional cross sections of volcanic plumes at various distances from the volcano. These reveal that the SO_2 plume actually has a larger cross section than that of the visible vapor plume. Discrete SO_2 plumes have been outlined at distances of greater than 80 km from the volcano.

We have previously used the COSPEC for determining the rate of SO_2 emission from volcanoes. In addition, we now calculate complete concentration profiles throughout the plume. The Interscan which directly measures SO_2 concentration has been used simultaneously with the COSPEC, the data intergrated, and compared with the COSPEC data. The results agree very well. Concentration distribution in cross sections of the Masaya, Nicaragua volcanic plume reveal areas of 0.4 ppm as far downwind as 37 km. In the actively rising eruption column directly over the vent of Santiaguito Dome, Guatemala SO_2 concentrations were >1.0 ppm.

V 134 INVITED PAPER

GAS ANALYSES OF AIRBORNE SAMPLES FROM ST. HELENS ERUPTION PLUME

D.R. Cronn (Air Pollution Research Section, Washington State University, Pullman, WA 99164)

Whole air gas samples have been collected in the numerous volcanic eruption plumes of Mt. St. Helens [illegible] steam and ash explosion of March [illegible] Airborne samples have been collected using [illegible] aircraft in collaboration with the University of Washington, Los Alamos Scientific Labs and the Department of Energy, and EPA Las Vegas. The samples have been analyzed for a variety of trace gases with emphasis on components such as COS, CS_2 and CO_2 which occur in volcanic emissions. After correction for sample transfer losses, COS levels ranged from 0.3 ppb to 2.5 ppb; CS_2 from 0.08 to 0.7 ppb. The trace gas levels will be related to concurrent measurements such as SO_2, H_2S and/or SO_4, as well as other flight parameters obtained by the various collaborators.

V 135 INVITED PAPER

COMPARISONS BETWEEN AIRBORNE MEASUREMENTS OF THE VOLCANIC EMISSIONS FROM MT. ST. AUGUSTINE 1976 AND MT. ST. HELENS 1980

P. V. Hobbs
L. F. Radke
D. A. Hegg
M. W. Eltgroth
J. P. Tuell (all at Cloud and Aerosol Research Group, Dept. of Atmos. Sci. AK-40, University of Washington, Seattle, WA 98195

Extensive airborne measurements have been obtained of the particles and gases emitted during the explosive eruptions of Mt. St. Augustine, Alaska, in 1976 and Mt. St. Helens, Washington, in 1980. These two geologically similar volcanoes both produced gas-rich tephra representing a range of source materials from andesite to dacite.

The Mt. St. Augustine eruption consisted of three periods of explosive vulcanism, each progressively weaker (January, February and April, 1976). Our measurements were made during February, followed by post-eruptive measurements in April, 1977. Our measurements of the Mt. St. Helen's eruption have covered the entire eruption sequence to date, including pre-eruptive, eruptive and intra-eruptive, and include several of the five major eruptions.

The size distributions of particles measured during the eruptions of both volcanoes are remarkably similar. In both cases the particles consist mainly of super-micron sized particles (with a small water soluble component).

Strongly acidic emissions, with a major sub-micron component, were characteristic of the intra-eruptive phases of both volcanoes.

The sulfur gases from Mt. St. Augustine remained largely SO_2 until more than a year after the initial eruptions. H_2S has remained a significant component of the sulfur emissions from Mt. St. Helens. However, the net sulfur fluxes from the volcanoes were generally similar.

Unlike Mt. St. Augustine, the NO_2 emissions from Mt. St. Helens have been occasionally significant (~7kg s^{-1}). When large amounts of trace gases were present, depletion of ozone was noted in the intra-eruptive plumes.

V 136 INVITED PAPER

MASAYA VOLCANO, NICARAGUA: A MAJOR SOURCE OF TROPOSPHERIC SO_2 DURING 1980 AND ITS IMPACT ON THE ADJACENT ENVIRONMENT

Stanley N. Williams[1]
Richard E. Stoiber[1]
N.M. Johnson[1]
W.E. Winner[2]
M.A. Parnell, Jr.[1]
D.J. Huebert[3]

The greatest natural contribution of SO_2 gas and aerosol to the troposphere in 1980 is believed to be the >0.5 x 10^6 mt emitted from Santiago Crater of Masaya Volcano, Nicaragua. In 1973 it was about 12% of this amount. SO_2 flux and the ratio of SO_2/HCl gas indicate an HCl contribution of >0.6 x 10^6 mt for 1980. The large continuous SO_2 emission which began in late 1979 is similar to events of about 25, 50, and 75 years ago, each of which lasted 5 to 10 years. Ground level SO_2 concentrations up to 0.6 ppm occur at 15 km downwind. Visual damage to cloud forest correlates with highest gas levels, yet perennial understory species appear healthy despite large amounts of SO_2 diffused through stomata. "Acid rain" beneath the plume has a range of pH from 2.6 to 3.9. It is largely neutralized by contact with herbaceous understory vegetation. Stream and springwater in the area presently show no acidification effects. In the soils, which are developed in Quaternary ashfall deposits, two acid neutralization processes appear to occur. The more effective process involves base leaching from exchange sites in base-rich soils (Mollic Vitrandepts) which produces relatively high soil pHs (6.24 - 7.28). A less effective process involves the dissolution of amorphous, aluminous phases (allophane) in the more poorly buffered soils (Typic Durandepts), which produces much lower soil pHs (4.51 - 5.58).

[1]Dept. of Earth Sciences, Dartmouth College, Hanover, NH 03755
[2]Dept. of Biological Sciences, Stanford Univ., Stanford, CA 94305
[3]Dept. of Chemistry, Colorado College, Colorado Springs, CO 80903

V 137 INVITED PAPER

GAS CHROMATOGRAPHIC DETERMINATION OF SOME CONSTITUENTS OF VOLCANIC GASES

P.D. Cadle (National Center for Atmospheric Research, Boulder, Colorado 80307)
L.E. Heidt (National Center for Atmospheric Research, Boulder, Colorado 80307)

Gas chromatographic analyses have been made of the gases emitted either as fume or eruption clouds from Pacaya, Fuego, and Santiaguito volcanoes in Guatemala; the Kilauea "Sulphur Bank" and Mauna Loa in Hawaii; and Mt. St Helens, during the early stages of its 1980 eruptive cycle, when the eruptions were largely or entirely phreatic.

Among the conclusions reached are that Mt. St. Helens erupted various magma gases even during the phreatic stages of the eruptions, that the methane often observed in volcanic gases is almost certainly of magma origin, and that volcanoes are only a minor source of carbonyl sulfide in the atmosphere.

*The National Center for Atmospheric Research is sponsored by the National Science Foundation.

V 138

COMPARISON OF AEROSOLS FROM ERUPTIONS OF SANTIAGUITO, GUATEMALA AND ST. HELENS

R. L. Chuan (Brunswick Corporation, Costa Mesa, CA, 92626)
D. C. Woods (NASA Langley Research Center, Hampton, VA 23665)

The results of direct airborne aerosol sampling of eruption clouds from Santiaguito in February, 1980, are compared with those in February, 1978. The multimodal (mostly tri-modal) nature of the aerosol size distribution appears to be generally the same, but the amount of sulfuric acid burden on the solid particles appears much less in 1980 than in 1978. There is no discernible (either by SEM imaging or electron-microprobing) mantle of acid on particles larger than about 5 μm in the 1980 eruption samples, while those from 1978 were literally mantled. The early, phreatic eruptions of St. Helens in April, 1980, were found to produce a nearly monomodal aerosol, with large (> 15 μm) plagioclase particles free of any acid. Even the very small number of sub-micron particles (constituting < 1% of the total aerosol mass) are free of acid mantling. By contrast, the aerosol from the premonitory emissions from St. Helens in August, 1980 (just preceding the August 7 eruption) was tri-modal, and the sub-micron mode particles were covered with sulfuric acid.

V 139

CHARACTERIZATION OF STRATOSPHERIC AEROSOLS IN ERUPTION PLUMES FROM MT. ST. HELENS

D. C. Woods (NASA Langley Research Center, Hampton, VA, 23665)
R. L. Chuan (Brunswick Corporation, Costa Mesa, CA, 92626)
(Sponsor: P. B. Russell)

Data on aerosol size distribution, concentration, morphology and composition have been obtained in the stratospheric clouds formed by effluents from the eruptions of Mt. St. Helens. A multistage inertial impactor, which classifies aerosols by size and measures the mass in each size interval by means of piezoelectric microbalances, was flown through the eruption cloud on the NASA Ames U-2 research aircraft along with other sampling instruments. Measurements were made on May 22, 1980, 4 days after the May 18 eruption, on May 27, 2 days after the May 25 eruption and in an aged plume, on June 17. The size distributions in the fresh plumes (May 22 and May 27) were found to be monomodal and very narrow in size band with most of the mass impacting in stages 7 and 6 of the cascade impactor corresponding to geometric mean particle diameters of 0.23 μm and 0.54 μm. These are quite different from the distributions obtained in the mild eruption plumes measured near the vents of St. Helens in April and August 1980 and from Santiaguito and Fuego in 1978 which were multimodal and covered a much broader size range. On the other hand, the size distribution in the aged stratospheric plume (June 17 measurement, probably from the May 18 eruption) was multimodal with peaks at about 0.02-μm, 0.1-μm and 1.3-μm diameter. Energy dispersive x-ray analysis show the particles in larger size range >1.0 μm to consist of silicates (mostly Si and Al) with some sulfuric acid, while the sub-micron size particles consist almost entirely of sulfuric acid droplets.

V 140 INVITED PAPER

BALLOON-BORNE AEROSOL MEASUREMENTS FOLLOWING THE ERUPTION OF MT. ST. HELENS

D.J. Hofmann
J. M. Rosen (both at: Department of Physics and Astronomy, University of Wyoming, Laramie, WY 82071)